
CONTROL OF THE POWER FLOWS OF A STOCHASTIC POWER SYSTEM

Zhen Wang ^{*},
Kaihua Xi [†], Aijie Cheng [†],
Hai Xiang Lin [‡], Jan H. van Schuppen [‡].

November 29, 2023

ABSTRACT

How to determine the power supply of a power system to guarantee that the state remains during a short horizon in a critical subset of the state set? The critical subset is related to the power flows of all power lines of a power system and to transient stability. The control objective is to minimize a cost function. That function is defined as the maximal power flow over all power lines, including a multiple of its standard deviation, as a function of the power supply vector. That the controlled system has an improved performance is shown by numerical results of three academic examples including an eight-node academic network, a twelve-node ring network, and a Manhattan-grid network.

Keywords and Phrases: power systems, control of the power flows, optimization of the power supply vector.

1 Introduction

The aim of this paper is to present the solution of a control problem for a power system which is subject to stochastic disturbances and which may be in danger of losing transient stability.

Motivation The motivation of this paper is the fact that current power systems experience fluctuations in power lines and that such fluctuations are expected to increase in intensity the coming decades. The fluctuations of the power flows are due to the power sources, in particular to the renewable power sources including wind turbines, wind parks, solar panels, photovoltaic panels, biomass generators, tidal energy, all without online CO_2 production. The power supply of wind turbines and photovoltaic panels will not be steady during short or long time scales, but fluctuate with the weather and other factors. The fluctuations due to power demand are expected to increase in intensity due to an increasing variety of power loads. The fluctuations of power flows of the power network endanger the transient stability of the power system, for which a form of control is needed, [13, 16].

Problem Introduction The main control objective in this paper is to maintain transient stability of the power system.

^{*}Zhen Wang is with the School of Mathematics, Shandong University, Jinan, 250100, Shandong Province, China and is visiting the Dept. of Applied Mathematics, Delft University of Technology, Delft, The Netherlands from November 2021 till February 2024 (email: wangzhen17@mail.sdu.edu.cn). Zhen Wang is grateful to the China Scholarship Council (No. 202106220104) for financial support for his stay at Delft University of Technology in Delft, The Netherlands.

[†]Kaihua Xi and Aijie Cheng are with the School of Mathematics, Shandong University, Jinan, 250100, Shandong Province, China (email: kxi@sdu.edu.cn, aijie@sdu.edu.cn).

[‡]Hai Xiang Lin and Jan H. van Schuppen are with the Dept. of Applied Mathematics, Delft University of Technology, Delft, The Netherlands (email: H.X.Lin@tudelft.nl, j.h.vanschuppen@tudelft.nl, vanschuppenjanh@freedom.nl).

The control of a power system is distinguished into three stages for different control horizons. Inspired by frequency control, the three phases are called: Primary Control, Secondary Control, and Tertiary Control. Secondary control concerns the periodic setting of power supply, with a period of the short horizon of between three and five minutes.

Secondary Control is the focus of this paper, with as main control objective keeping the state trajectory inside a critical subset of the state set. It is a generalization of secondary frequency control in that the control objective is not only that power supply equals power demand, but also that the power supply improves transient stability by minimization of the effects of stochastic disturbances. The behavior of the state of a power system best remains inside the domain of attraction of a strictly stable synchronous state, defined below, for which a related condition is that the state remains in a critical subset of the state set.

Problem Synthesize a control law for the power supply vectors such that the controlled power system satisfies that the power flows of the power system all belong to a critical subset, with a prespecified probability. That subset is defined by the condition that, for all power lines, the phase-angle difference over a power line remains in the interval $(-\pi/2, +\pi/2)$. In particular, a stochastic control problem will be formulated in which the control objective is to control the probability distribution of the power flows such that the probability of exiting the critical subset is less than a prescribed threshold.

Literature Review The power system is adjusted from [19] and [14]. The literature on stability of a nonlinear power systems, include [42] in which J. Zaborszky et al. analysed the stable region and the stability boundary of a power system and [5] in which H. Chiang et al. introduced a method to estimate stability regions for general nonlinear dynamical systems.

Stability of a linear power system, which is also called small signal stability, is discussed by P. Menck et al who used what is called the basin stability to measure linear stability [24]. After the formulation of this metric, they used a Monte Carlo method to measure the basin stability and they found that the dead tree structure may ruin the synchronous stability [23]. The dead tree can be cured by adding transmission lines, but meanwhile a paradoxical phenomenon [37] may occur. What is more, the impact of the grid structure has also been analysed in [35], in which the power system is subjected to stochastic disturbances. Furthermore, A. Motter et al used the second largest eigenvalue to investigate the stability region of linearized power systems, which can be enlarged by tuning generator parameters [25].

Recent literature on secondary frequency control, include N. Li et al who designed an algorithm which integrated economic cost into automatic generation control, meanwhile keeping the former decentralized structure in [21], F. Dörfler et al who put forward a method between centralized and distributed control based on continuous-time feedback control called Gather and Broadcast control to restore frequency in [8], and K. Xi et al who designed a method called Power Imbalance Allocation Control to avoid overshoots and the frequency deviation with a small control cost in [40], where transient performance can be improved through an accelerated convergence speed [39].

Recent publications on the integration of renewable sources, include [22] in which E. Marris introduced a management with power supply and demand, and how the future power system would be like, from which one learns that renewable sources will replace the traditional generation gradually in the future and therefore the inertia will dramatically drop down to zero after the penetration of these renewable sources, [27] in which B. Poola et al put forward an algorithm on where to place virtual inertia aiming to optimize a \mathcal{H}_2 norm which is a global metric containing both phase-angle difference and frequency deviation, [31] in which E. Tegling et al also used \mathcal{H}_2 norm to evaluate the resistive power losses in terms of design of future power systems where more generators and transmission lines should be accommodated.

Research on the spread of the fluctuations caused by disturbances in power systems, include [2] in which S. Auer et al simulated the spread on frequency deviation in a tree-like network with fluctuations at particular node in order to predict the most effected region, [45] in which X. Zhang et al formulated a theoretical result for the dynamical response with an external signal input with distributed signals and it satisfies linear superposition principle, [44] the same authors as in previous publication further proposed a master function which can be numerically estimated through an analytically defined topological factor to predict the arrival time of perturbations.

However, few papers have investigated analytically the stochastic fluctuations of power systems and their control. Even fewer papers presented concrete procedures to suppress or to mitigate the fluctuations of a power system with integrated renewable sources.

Contributions of this Paper (1) Analysis of a stochastic power system and the formulation of a control objective function for secondary control of a stochastic linearized power system. (2) The main contribution, numerical results for the optimal power supply vectors and of the power line flows for three academic examples, including a particular

eight-node example, a twelve-node ring network, and a small Manhattan-grid example. These three examples are chosen so as to investigate the influence of different network structures on the transient stability.

Paper Organization Section 2 introduces a deterministic power system and a stochastic linearized power system. The control objective function is introduced and defined in Section 3. The performance of the controlled power systems for three illustrative examples, based on their numerical computations, are summarized and displayed in Section 4. Section 5 states conclusions and describes open research issues. The reader may find results on a related optimization problem in the companion paper [36].

2 The Power System

2.1 Notation

The set of the integers is denoted by \mathbb{Z} and that of the positive integers by $\mathbb{Z}_+ = \{1, 2, \dots\}$. The natural numbers are denoted by $\mathbb{N} = \{0, 1, 2, \dots\}$. For any positive integer $k \in \mathbb{Z}_+$ denote the finite sets $\mathbb{Z}_k = \{1, 2, \dots, k\}$ and $\mathbb{N}_k = \{0, 1, 2, \dots, k\}$. The real numbers, the positive real numbers, and the strictly positive real numbers are respectively denoted by \mathbb{R} , $\mathbb{R}_+ = [0, \infty)$, and $\mathbb{R}_{s+} = (0, \infty)$. The complex numbers are denoted by \mathbb{C} . The open left part of the complex plane is denoted by $\mathbb{C}_o^- = \{c \in \mathbb{C} \mid \text{Re}(c) < 0\}$. Define the notation for the *sign* function, $\text{sign}(x) = +1$, if $x > 0$, $= -1$ if $x < 0$, $= 0$, otherwise.

The vector space of $n \in \mathbb{Z}_+$ tuples of the real numbers is denoted by \mathbb{R}^n . Denoted by e_k the k^{th} unit vector whose k^{th} component equals one while the other components equal zeros. The set of matrices of size $n \times m$ with entries in the real numbers, is denoted by $\mathbb{R}^{n \times m}$. The set of matrices of size $n \times n$ with elements in the real numbers whose off-diagonal elements are all zeros is denoted by $\mathbb{R}_{diag}^{n \times n}$. Denote a diagonal matrix, with on the diagonal the elements of the vector $v \in \mathbb{R}^n$, by $\text{diag}(v) \in \mathbb{R}^{n \times n}$. A matrix $Q \in \mathbb{R}^{n \times n}$ is called *symmetric and positive definite* if for all $v \in \mathbb{R}^n$, $v^T Q v \geq 0$ and denote the set of those matrices by $\mathbb{R}_{pds}^{n \times n}$. Such a matrix is called *strictly positive definite* if, for all $v \in \mathbb{R}^n$ with $v \neq 0$, $v^T Q v > 0$ and denote the set of such matrices by $\mathbb{R}_{spds}^{n \times n}$.

The spectrum of the square matrix $A \in \mathbb{R}^{n \times n}$ is denoted by $\text{spec}(A)$, which set is defined as the set of eigenvalues of that matrix. Denote the *spectral index* of matrix $A \in \mathbb{R}^{n \times n}$ as the tuple $n_{si}(A) = \{n_-, n_0, n_+\}$ where $n_- \in \mathbb{N}$ is the number of eigenvalues with strictly negative real part, thus in $\mathbb{C}_o^- = \{c \in \mathbb{C} \mid \text{Re}(c) < 0\}$, $n_0 \in \mathbb{N}$ is the number of eigenvalues with real part equal to zero, and $n_+ \in \mathbb{N}$ is the number of eigenvalues with strictly positive real part, thus in $\mathbb{C}_o^+ = \{c \in \mathbb{C} \mid \text{Re}(c) > 0\}$.

The symbol $x \in G(m_x, Q_x)$ denotes that the random variable $x : \Omega \rightarrow \mathbb{R}^n$ has a Gaussian probability distribution function with mean $m_x \in \mathbb{R}^n$ and variance $Q_x \in \mathbb{R}_{pds}^{n \times n}$.

2.2 The Deterministic Nonlinear Power System

The *power system* is defined by a set of nonlinear differential equations driven by the input signal p , [19], [14], [1], and [6]. The *nominal frequency* is defined to be the frequency of a rotating frame with respect to which the actual power system will be defined. The value of the nominal frequency equals 50 Hz in Europe and in Asia, and equals 60 Hz in North America.

The graph of the power network is described by the tuple $(\mathcal{V}, \mathcal{E})$, where \mathcal{V} is the set of nodes and \mathcal{E} is the set of lines. Denote by $n_{\mathcal{E}}$ the number of lines and by $n_{\mathcal{V}}$ the number of nodes. It is assumed that the undirected graph of the power network is connected, meaning that for every tuple $(i, j) \in \mathcal{E}$, there exists a path from i to j .

The system is specified by the following equations,

$$\frac{d\theta(t)}{dt} = \omega(t), \theta(0) = \theta_0, \quad (1)$$

$$M \frac{d\omega(t)}{dt} = -D\omega(t) - BWf_d(\theta(t)) + p(t), \omega(0) = \omega_0; \quad (2)$$

$$\Leftrightarrow \forall i \in \mathcal{V},$$

$$\frac{d\theta_i(t)}{dt} = \omega_i(t), \theta_i(0) = \theta_{i,0}, \quad (3)$$

$$M_{i,i} \frac{d\omega_i(t)}{dt} = -D_{i,i}\omega_i(t) + \sum_{j \in \mathcal{V}, (i,j) \in \mathcal{E}} L_{i,j} \sin(\theta_i(t) - \theta_j(t)) + p_i(t), \quad (4)$$

$$\omega_i(0) = \omega_{i,0}, \text{ where,}$$

$$T = [0, +\infty),$$

$$f_d(\theta) = (\sin(\theta_{i_k} - \theta_{j_k}), \forall k = (i_k, j_k) \in \mathcal{E}) = \sin(B^\top \theta) \in \mathbb{R}^{n_\mathcal{E}}; \text{ which satisfies that,} \quad (5)$$

$$\forall \theta \in \mathbb{R}^{n_\mathcal{V}}, \forall \psi \in \mathbb{R},$$

$$f_d(\theta) = f_d(\theta + \psi \times \mathbf{1}_{n_\mathcal{V}});, \quad (6)$$

$$\mathbf{1}_{n_\mathcal{V}} = [1 \ 1 \ \cdots \ 1]^\top \in \mathbb{R}_{s+}^{n_\mathcal{V}},$$

$$M \in \mathbb{R}_{\text{diag}}^{n_\mathcal{V} \times n_\mathcal{V}}, \forall i \in \mathbb{Z}_{n_\mathcal{V}}, M_{i,i} > 0;$$

$$D \in \mathbb{R}_{\text{diag}}^{n_\mathcal{V} \times n_\mathcal{V}}, \forall i \in \mathbb{Z}_{n_\mathcal{V}}, D_{i,i} \geq 0;$$

$$B \in \mathbb{R}^{n_\mathcal{V} \times n_\mathcal{E}}, L \in \mathbb{R}^{n_\mathcal{V} \times n_\mathcal{V}}, W \in \mathbb{R}_{\text{diag}}^{n_\mathcal{E} \times n_\mathcal{E}},$$

$$B_{i,k} = \begin{cases} +1, & \text{if } k = (i, j_k) \in \mathbb{Z}_{n_\mathcal{E}}, \\ -1, & \text{if } k = (j_k, i) \in \mathbb{Z}_{n_\mathcal{E}}, \\ 0, & \text{else;} \end{cases}$$

$$L_{i,j} = \begin{cases} b_{i,j} \hat{V}_i \hat{V}_j, & \text{if } (i, j) \in \mathcal{E}, \\ 0, & \text{else;} \end{cases}$$

$$W_{k,k} = L_{i_k, j_k} > 0, \text{ if } k = (i_k, j_k) \in \mathcal{E};$$

where $L_{i,j} = b_{i,j} \hat{V}_i \hat{V}_j$ is the effective capacity of line $(i, j) \in \mathcal{E}$, in which \hat{V}_i is the voltage at node i and $b_{i,j}$ is the susceptance of line (i, j) , the dynamics of the voltage is neglected in the short horizon, and $L_{i,j}$ is considered as a constant on this horizon.

Call $\theta : T \rightarrow \mathbb{R}^{n_\mathcal{V}}$ the *phase deviation vector*, $\omega : T \rightarrow \mathbb{R}^{n_\mathcal{V}}$ the *frequency deviation vector* (θ, ω are relative to the nominal frequency), $p = [p^+, -p^-]^\top : T \rightarrow \mathbb{R}^{n_\mathcal{V}}$ the *power vector*, $p^+ : T \rightarrow \mathbb{R}^{n^+}$ the *vector of power supplies*, $p^- : T \rightarrow \mathbb{R}^{n_\mathcal{V} - n^+}$ the *vector of power loads*, $M \in \mathbb{R}_{s+}^{n_\mathcal{V} \times n_\mathcal{V}}$ the *matrix of inertias*, $D \in \mathbb{R}_{s+}^{n_\mathcal{V} \times n_\mathcal{V}}$ the *matrix of damping constants*, $L \in \mathbb{R}_{s+}^{n_\mathcal{E} \times n_\mathcal{E}}$, the *matrix of power line capacities*, k is the index of line (i_k, j_k) , $B \in \mathbb{R}^{n_\mathcal{V} \times n_\mathcal{E}}$, the *incidence matrix*, where the directions of the lines are consistently specified, and call $f_d \in \mathbb{R}^{n_\mathcal{E}}$ the *vector of sines of the phase-angle differences across power lines*. It is assumed that for all initial conditions there exists a unique solution of the differential equation of the power system. Denote by $(\theta(t; 0, \theta_0), \omega(t; 0, \omega_0))$ for all times $t \in T$, the solution of the differential equation where the state at time $t \in T$ is denoted by $(\theta(t), \omega(t))^T$.

2.3 The Synchronous State

Consider the power system described in Section 2.2. A short while after the start of the short horizon, the electric machines will run steady. One calls such a state a synchronous state instead of a steady state. In the power network, we suppose a subset of the nodes provide only power supply and a complementary subset have only power demand. The nodes are labeled such that:

$$p(t) = \begin{bmatrix} p^+(t) \\ -p^-(t) \end{bmatrix} \Leftrightarrow p^+(t) = [p_1^+(t) \ \cdots \ p_{n^+}^+(t)]^\top,$$

$$p^-(t) = [p_{n^++1}^-(t) \ \cdots \ p_{n_\mathcal{V}}^-(t)]^\top,$$

which means that the nodes $1 \rightarrow n^+$ have only power supply and the nodes $n^+ + 1 \rightarrow n_V$ have only power demand. Consider a steady power supply vector $p_{sp} \in \mathbb{R}^{n_V}$. Recall that θ and ω are defined with respect to a frame rotating at the nominal frequency. A *synchronous state* is defined as a tuple $(\theta_s, \omega_s 1_{n_V}) \in \mathbb{R}^{2n_V}$ with $\omega_s \in \mathbb{R}$, which satisfy the *synchronous state equations*,

$$\begin{aligned} 0 &= -D1_{n_V}\omega_s - BWf_d(\theta_s) + p_{sp}, \quad \omega_s 1_{n_V} = 0 \Leftrightarrow \\ 0 &= -D_{(i,i)}\omega_s - \sum_{j=1}^{n_V} L_{i,j} \sin(\theta_{s,i} - \theta_{s,j}) + p_{sp,i}, \quad 0 = \omega_s. \end{aligned} \quad (7)$$

2.4 The Existence of a Critical-Stable Synchronous State

Assumption 2.1 *It is assumed that there exists a synchronous state $(\theta_s, \omega_s 1_{n_V})$, which satisfies the condition that $(\theta_{s,i_k} - \theta_{s,j_k}) \in (-\pi/2, +\pi/2)$, for all $(i_k, j_k) \in \mathcal{E}$ and $\omega_s = 0$. That state will be referred to as a critical-stable synchronous state.*

The assumption can in practice be met by a reduction of the power demand to a lower value. If a critical-stable synchronous state exists then it is unique, [28].

The synchronous state is a solution of the synchronous state equation (7). The solvability of this equation has received much attention in the literature, [3], [15], [7], [28]. Below we use a solution procedure from the literature.

Theorem 2.2 [7]. *Consider the power system specified in Section 2.2. There exists a unique critical-stable synchronous state if there exists a $\gamma \in (0, \pi/2)$ such that,*

$$\|B^\top (BWB^\top)^\dagger p_{sp}\|_\infty \leq \sin(\gamma). \quad (8)$$

2.5 The Domain of the Power Supply Vector

Definition 2.3 The domain of the power supply vector.

Consider the maximal power supply and the power demand for the next short horizon, denoted respectively by $p^{+,max} \in \mathbb{R}_+^{n^+}$ and $p^- \in \mathbb{R}_+^{n^-}$. Define then $p_{sum}^{+,max} = \sum_{i=1}^{n^+} p_i^{+,max}$ and $p_{sum}^- = \sum_{i=1}^{n^-} p_i^-$. Note that p_{sum}^- is strictly positive.

Construct a power supply vector $p^+ \in \mathbb{R}^{n^+}$ according to the following steps,

- (1) choose $p_{sum}^+ \in \mathbb{R}$ such that $p_{sum}^+ = p_{sum}^-$,
- (2) choose $p_i^+ \in [0, p_i^{+,max}]$, $\forall i = 1, 2, \dots, n^+ - 1$,

$$\text{and set } p_{n^+}^+ = p_{sum}^+ - \sum_{i=1}^{n^+-1} p_i^+;$$

- (3) p^+ has to satisfy that $\forall j \in \mathbb{Z}_{n^+}$,

$$p_{sum}^+ - \sum_{i=1, i \neq j}^{n^+} p_i^+ \in [0, p_j^{+,max}].$$

The latter conditions denote that: (1) the power supply of p^+ equals the power demand; (2) the power supply components $p_1^+, p_2^+, \dots, p_{n^+-1}^+$ are feasible; (3) the power supply vector p^+ satisfies these conditions.

Define the *decision vector* as a subvector of the power supply vector, by the formula

$$p_s = [p_1^+ \quad p_2^+ \quad \dots \quad p_{n^+-1}^+] \in \mathbb{R}^{n^+-1}.$$

Define the *domain of the decision vector* as the set P^+ , where the matrices A_1, b_1, b_2 are provided in Appendix .2.1,

$$\begin{aligned} P^+ &= P^+(p^{+,max}, p^-) \\ &= \left\{ p_s \in \mathbb{R}_+^{n^+-1} \mid \text{conditions (1), (2), (3) above} \right. \\ &\quad \left. \text{all hold, and } b_1 \leq A_1 p_s, p_s \leq b_2. \right\}. \end{aligned}$$

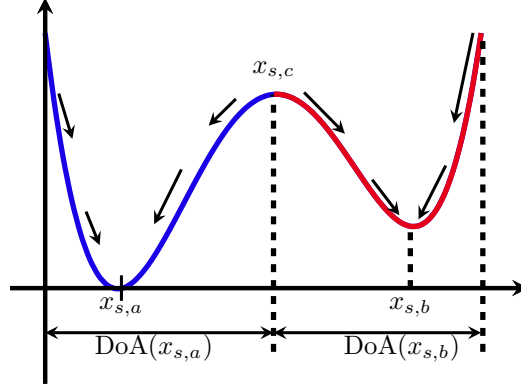


Figure 1: Two stable points $x_{s,a}$ and $x_{s,b}$ with their domain of attraction and a saddle point $x_{s,c}$

Assumption 2.4 Assume that the available power supply is larger than or equal to the power demand, $p_{sum}^{+,max} \geq p_{sum}^-$.

The condition that power supply p_{sum}^+ equals the power demand and that the synchronous state equation (7) holds, imply that the synchronous frequency ω_s equals zero.

Proposition 2.5 The domain P^+ is compact and convex. Moreover, it is a polytope.

2.6 Linearize the Power System at the Synchronous State

The procedure to linearize the deterministic nonlinear power control system at a critical-stable synchronous state may be found in the references [42] and [25].

$$\begin{aligned} \frac{dz(t)}{dt} &= J(\theta_s, 0)z(t) + \begin{bmatrix} 0 \\ I \end{bmatrix} \Delta p(t), & (9) \\ z(0) &= \begin{bmatrix} \theta(0) - \theta_s \\ \omega(0) - 0 \end{bmatrix}, \quad \Delta p(t) = p(t) - p_{sp}, \\ z(t) &= \begin{bmatrix} \Delta \theta(t) \\ \Delta \omega(t) \end{bmatrix} = \begin{bmatrix} \theta(t) - \theta_s \\ \omega(t) - \omega_s \end{bmatrix}, \\ J(\theta_s, 0) &= \begin{bmatrix} 0 & I_{n_\nu} \\ -M^{-1}BWF(\theta_s) & -M^{-1}D \end{bmatrix}, & (10) \\ F(\theta_s) &= \left(\frac{df_d(\theta)}{d\theta} \right) \Big|_{\theta=\theta_s} \in \mathbb{R}^{n_\nu \times n_\nu}. \end{aligned}$$

where the matrix of equation (10) is called the *Jacobian matrix* and the product $BWF(\theta_s)$ is called the *Laplacian matrix* of the power network. The reader finds in Appendix .1 the Laplacian matrix of a complete power network.

The Laplacian matrix of the power network is in general a singular matrix, [35]. For all of the examples of Section 4 there is one eigenvalue at zero. The eigenvalues of the Jacobian matrix of a power system with a complete power network, are discussed in [28, 41].

2.7 The Transient Stability of a Nonlinear Power System

The reader finds in this subsection the concepts of the domain of attraction of a synchronous state and the definition of transient stability of a power system. For concepts and a classification of power system stability, see [19]. The main basis for this subsection are the papers on stability of nonlinear power systems, [42] and [4].

Definition 2.6 Define the domain of attraction of a critical-stable synchronous state, $(\theta_s, \omega_s \mathbf{1}_{n_\nu}) \in \mathbb{R}^{2n_\nu}$, of a deterministic nonlinear power system as a subset of the state set such that the state trajectory of the power system, starting at any state of this subset, will converge to the considered synchronous state; in terms of mathematical

notation,

$$\begin{aligned} \text{DoA}(\theta_s, \omega_s) &= \left\{ \begin{array}{l} (\theta_0, \omega_0) \in \mathbb{R}^{2n\nu} \mid \lim_{t \rightarrow +\infty} \\ (\theta(t; 0, (\theta_0, \omega_0)), \omega(t; 0, (\theta_0, \omega_0))) \\ = (\theta_s, (\omega_s \times \mathbf{1}_{n\nu})) \end{array} \right\}. \end{aligned}$$

Call the dynamic behavior of the power system at the critical-stable synchronous state x_s during a short horizon transient stable if (1) $\text{spec}(J(\theta_s, 0)) \setminus \{0\} \subset \mathbb{C}^-$ and (2) the state trajectory remains inside the open domain of attraction $\text{DoA}(x_s)$ during the considered short horizon.

An example with domains of attraction is displayed in Fig. 1. The figure displays an abstract energy function as a function of a one-dimensional state. Seen are the open domains of attraction of the two steady states $x_{s,a}$ and $x_{s,b}$ and the steady state $x_{s,c}$ whose domain of attraction is only the steady state itself.

In engineering power systems a deterministic nonlinear power system, at a critical-stable synchronous state, is often subject to disturbances. Then the state trajectory of such a system will fluctuate in the domain of attraction and will often return to a neighborhood of the synchronous state. Due to particular disturbances, the state trajectory may leave the domain of attraction and move into the domain of another synchronous state where its dynamic behavior may be different. The reader is referred to the papers [42], [4] for this dynamic behavior. A departure from the domain of a selected synchronous state has to be avoided during the operation of a power system.

2.8 The Stochastic Linearized Power System

A stochastic power system is formulated based on the linearized power system. The deterministic functions (θ, ω) are now modified into stochastic processes. The difference Δp of the power supply and the power demand from their values at the synchronous state on a short horizon, is modeled as a Brownian motion process. The stochastic linearized power system is then defined by the linear stochastic differential equation, [17], [20],

$$dx(t) = J(\theta_s, 0) x(t) dt + K dv(t), x(0), \quad (11)$$

$$y(t) = Cx(t), \quad (12)$$

$$x : \Omega \times T \rightarrow \mathbb{R}^{n\nu}, y : \Omega \times T \rightarrow \mathbb{R}^{n\varepsilon},$$

$$x(t) = \begin{bmatrix} \theta(t) \\ \omega(t) \end{bmatrix}, K = \begin{bmatrix} 0 \\ K_2 \end{bmatrix} \in \mathbb{R}^{2n\nu \times n\nu},$$

$$C = [B^\top \quad 0] \in \mathbb{R}^{n\varepsilon \times 2n\nu},$$

where (Ω, F, P) denotes a probability space consisting of a set Ω , a σ -algebra F , and a probability measure P ; $T = [0, \infty)$ denotes the time index set; $x(0) : \Omega \rightarrow \mathbb{R}^{2n\nu}$ denotes the initial state of the stochastic system which is assumed to have a Gaussian distribution with expectation $m_{x(0)} \in \mathbb{R}^{2n\nu}$ and a symmetric positive definite variance matrix $Q_{x(0)} \in \mathbb{R}_{spd}^{2n\nu \times 2n\nu}$, hence $x(0) \in G(m_{x(0)}, Q_{x(0)})$; $v : \Omega \times T \rightarrow \mathbb{R}^{n\nu}$ denotes a Brownian motion process such that $\forall s, t \in T, s < t, v(t) - v(s) \in G(0, (t-s) \times I_{n\nu})$, while $F^{x(0)}, F_\infty^v$ are independent σ -algebras; $K_2 \in \mathbb{R}_{diag}^{n\nu \times n\nu}$ denotes a matrix which multiplies the vector valued Brownian motion, which is a diagonal matrix with $K_2(i, i) \geq 0, \forall i \in \mathbb{Z}_{n\nu}$.

Definition 2.7 Consider the stochastic linearized power system and consider a synchronous state $x_s = (\theta_s, \omega_s \mathbf{1}_{n\nu})$ which satisfies Assumption 2.1. Define the critical subset X_c as a subset of the state set,

$$\Theta_c = \left\{ \begin{array}{l} \theta \in \mathbb{R}^{n\nu} \mid \forall k = (i_k, j_k) \in \mathcal{E}, \\ (\theta_{i_k} - \theta_{j_k}) \in (-\pi/2, +\pi/2) \end{array} \right\},$$

$$X_c = \Theta_c \times \mathbb{R}^{n\nu} \subset \mathbb{R}^{2n\nu}.$$

Call the dynamic behavior of the power system at the critical-stable synchronous state x_s during a short horizon and for a prespecified value $\epsilon \in (0, 1)$, (probabilistically) critical-stable if (1) $\text{spec}(J(\theta_s, 0)) \setminus \{0\} \subset \mathbb{C}_\epsilon^-$ and (2) the probability is higher than $(1 - \epsilon) \in (0, 1)$ that the state trajectory, when started inside the critical subset, remains inside the critical subset $X_c = \Theta_c \times \mathbb{R}^{n\nu}$ during that short horizon.

In this paper attention is restricted to the condition that the power system is critical-stable on a short horizon. It is conjectured that this property implies that then the system is transient stable during the same short horizon.

In the literature there are necessary and sufficient conditions for stability of the synchronous state of a deterministic nonlinear power system, which is often condition (1) of transient stability. However, the understanding of the paper of J. Zaborszky et al., [41], in which monitoring of a power system is described, is that if conditions (1) and (2) of critical-stability holds, then condition (2) of transient stability also holds and the behavior of the nonlinear power system during a short horizon is transient stable.

2.9 The Invariant Distribution of the Linearized Stochastic Power System

It follows from [17, Theorem 6.17] and [20, Theorem 1.52] that x and y are Gaussian processes with for all times $t \in T$, $x(t) \in G(m_x(t), Q_x(t))$ and $y(t) \in G(m_y(t), Q_y(t))$.

If the Jacobian matrix $J(\theta_s, 0)$ is Hurwitz, hence $\text{spec}(J(\theta_s, 0)) \subseteq \mathbb{C}_o^-$, the following properties of the mean value and the variance matrix hold,

$$\begin{aligned} 0 &= \lim_{t \rightarrow \infty} m_x(t), & 0 &= \lim_{t \rightarrow \infty} m_y(t), \\ Q_x &= \lim_{t \rightarrow \infty} Q_x(t), & Q_y &= \lim_{t \rightarrow \infty} Q_y(t), \end{aligned}$$

and where Q_x is the unique solution of the following Lyapunov equation and Q_y satisfies,

$$0 = J(\theta_s, 0)Q_x + Q_x J(\theta_s, 0)^\top + K K^\top, \quad (13)$$

$$Q_y = C Q_x C^\top. \quad (14)$$

But in fact, the system matrix $J(\theta_s, 0)$ is not Hurwitz because the Laplacian matrix $BWF(\theta_s)$ has a zero eigenvalue. Therefore, there is a need for a reduction procedure, see [35].

Assumption 2.8 1. Recall Assumption 2.1. Assume in addition that the diagonal matrix K has strictly positive diagonal elements, hence, for all $k \in \mathcal{V}$, $K_{k,k} > 0$.

2. $(J(\theta_s, 0), K)$ is a controllable pair.

Assumption 2.8 with Condition (1) and the condition on the graph of the power network imply that Condition (2) holds.

Proposition 2.9 Assume that either Condition (1) or Condition (2) of Assumption 2.8 holds. Then, for any power line $k \in \mathbb{Z}_{n_\mathcal{E}}$ and any fixed power supply vector $p_s \in P^+$, the standard deviation $\sigma_k(p_s)$ is strictly positive; in terms of notation, $\sigma_k(p_s) = (Q_{y,(k,k)}(p_s))^{1/2} > 0$.

The proof of the above proposition may be found in Appendix .1.2.

From the discussion above follows that the random variable of the phase-angle difference over power line k of the power network, $\theta_{i_k}(t) - \theta_{j_k}(t)$, has the invariant Gaussian probability distribution, $\forall t \in T$ and $\forall k = (i_k, j_k) \in \mathcal{E}$,

$$\begin{aligned} \theta_{i_k}(t) - \theta_{j_k}(t) &\in G(m_k(p_s), \sigma_k(p_s)); \\ m_k(p_s) &= \theta_{s,i_k}(p_s) - \theta_{s,j_k}(p_s), \\ \sigma_k(p_s) &= Q_{y,(k,k)}(p_s)^{1/2} > 0; \text{ then,} \\ \frac{\theta_{i_k}(t) - \theta_{j_k}(t) - m_k(p_s)}{\sigma_k(p_s)} &\in G(0, 1); \\ \epsilon &= \int_{-\infty}^{r_\epsilon} p_{G(0,1)}(w) dw. \end{aligned}$$

See Table 1 for the relation between the threshold values and the values of the parameter, (ϵ, r_ϵ) , of $G(0, 1)$.

2.10 Towards the Control Objective Function

The computational complexity of the control objective function is to be reduced. The control objective function will be defined in Subsection 3.2. It aims at keeping the state of the stochastic linearized power system during a short horizon in the critical subset of the state set.

The probabilities that the maximum of a stationary Gaussian process on a finite interval is larger than a particular threshold, are available in the literature, see for example [11, Section 6.5]. However, even for a Brownian motion process the probabilities are expressed as an infinite series of integrals over Gaussian density functions. Such expressions require approximations which are computationally intensive. Therefore it has been decided to restrict attention to the probability at a particular time that the process exits the critical set according to the invariant probability distribution.

ϵ	r_ϵ
0.050	-1.65
0.040	-1.76
0.030	-1.89
0.020	-2.06
0.010	-2.33
0.001	-3.08

Table 1: Relation of probabilities and thresholds of a Gaussian probability distribution with mean zero and variance one. Thus, if $x \in G(0, 1)$ and $\epsilon \in (0, 1)$ then $P(\{x \leq r_\epsilon\}) \leq \epsilon$ and r_ϵ is an approximation of the maximal such real number.

Proposition 2.10 Consider the stochastic power system.

(a) The probability that the power flow of any power line exits the critical subset according to the invariant distribution of the vector of power line flows, equals,

$$\begin{aligned}
& \forall k \in \mathbb{Z}_{n_\epsilon}, \forall p_s \in P^+, \\
& p_{outc,k}(p_s) \\
& = P(\{\nu \in \Omega \mid \theta_{i_k}(\nu, t) - \theta_{j_k}(\nu, t) \leq -\pi/2\}) + \\
& \quad + P(\{\nu \in \Omega \mid \theta_{i_k}(\nu, t) - \theta_{j_k}(\nu, t) \geq +\pi/2\}) \\
& = f_{G(0,1)}(r_{a,k}(p_s)) + f_{G(0,1)}(-r_{b,k}(p_s)), \\
r_{a,k}(p_s) & = \frac{-\pi/2 - m_k(p_s)}{\sigma_k(p_s)}, \\
-r_{b,k}(p_s) & = \frac{-\pi/2 + m_k(p_s)}{\sigma_k(p_s)}; \\
r_{a,b,k}(p_s) & = \max\{r_{a,k}(p_s), -r_{b,k}(p_s)\}, \text{ then,} \\
r_{a,b,k}(p_s) & = \frac{-\pi/2 + |m_k(p_s)|}{\sigma_k(p_s)}.
\end{aligned}$$

(b) A lower bound. If $r_{a,b,k}(p_s) \leq r_{\epsilon/2}$ then $p_{outc,k}(p_s) \leq \epsilon$.

The proof of this proposition can be found in Appendix .1.3. Infimization of the lower bound derived above leads to the following alternative optimization criteria,

$$\begin{aligned}
(a) \quad & \inf_{p_s \in P^+} \max_{k \in \mathbb{Z}_{n_\epsilon}} r_{a,b,k}(p_s) \\
& = \inf_{p_s \in P^+} \max_{k \in \mathbb{Z}_{n_\epsilon}} \left(\frac{-\pi/2 + |m_k(p_s)|}{\sigma_k(p_s)} \right); \\
(b) \quad & \inf_{p_s \in P^+} \max_{k \in \mathbb{Z}_{n_\epsilon}} \left(\frac{|m_k(p_s)|}{\sigma_k(p_s)} - r_\epsilon \right) \\
& = \inf_{p_s \in P^+} \max_{k \in \mathbb{Z}_{n_\epsilon}} \left(\frac{|m_k(p_s)| - r_\epsilon \sigma_k(p_s)}{\sigma_k(p_s)} \right); \\
(c) \quad & f_d^* = \inf_{p_s \in P^+} \max_{k \in \mathbb{Z}_{n_\epsilon}} [|m_k(p_s)| - r_\epsilon \sigma_k(p_s)], \\
& \text{where } r_\epsilon \in (-\infty, 0).
\end{aligned}$$

Below optimization criterion (c) will be used. The criteria (a) and (b) involve division by σ_k which involves computational issues that are best avoided. The reader finds in Appendix .2 a description of two alternative criteria not used by the authors because of their computational complexity.

Note that $f_d^* \leq \pi/2$ implies that there exists a supply vector $p_s \in P^+$ such that $p_{outc}(p_s) \leq 2\epsilon$. This follows directly from Proposition 2.10.(b).

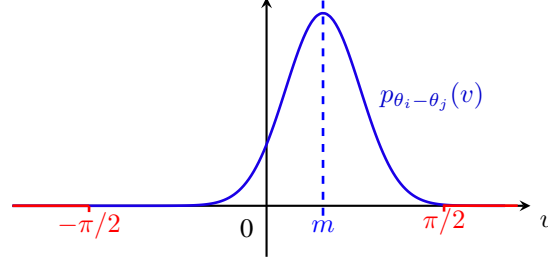


Figure 2: The probability density function of the phase-angle difference $(\theta_{i_k} - \theta_{j_k})$ of the power flow in power line $k = (i_k, j_k) \in \mathcal{E}$; and two red bars for the probabilities that the phase-angle difference is larger than $+\pi/2$ or less than $-\pi/2$. The parameters of the probability density function displayed are $(m, \sigma) = (0.4995, 0.3344)$ which values are chosen identical to those of Fig. 9 for ‘without control’.

3 The Control Problem

3.1 Introduction to the Control Problem

The setting of the problem is secondary control. The horizon is partitioned into a sequence of short horizons. A short horizon is typically three to five minutes.

This secondary control problem is a *generalization* of the secondary frequency control problem because its goals are: (1) power supply equals power demand (as in secondary frequency control); and (2) the probability that any of the power flows leaves the critical set during the next short horizon, is less than a prespecified threshold ϵ .

The control actuation will be as in secondary frequency control. The input of the power system determines the power supply of all power sources and that power supply is then kept constant during a short horizon. Output feedback is not used.

The *control objectives* are properties of the closed-loop controlled system which an engineer would like to attain. The main control objectives of this paper are: (1) the *delivery of electric power* to nodes with power demand, (2) the *transient stability* during each short horizon, (3) *acceptable transient behavior* during each short horizon, and (4) *minimization of the economic cost* of the power supply. The main operational control objective is transient stability of a power system as has been defined in Def. 2.6.

Restriction to critical subset of the state set. In stead of requiring that the state of the power system remains in the domain of attraction, attention is restricted to keeping the state of the power system in the critical subset of the state set. The literature on the relation of the critical subset and stability of a deterministic power system includes [28], [43], [41] and [33, Lemma 5.2]. It is an open research issue to provide a statement and proof which justifies this restriction.

Probability that the state of the system leaves the critical set. The control objective chosen leads therefore to the probability that, during a short horizon, the vector of phase-angle differences of the power flows of any power line leave the critical subset $X_c = \Theta_c \times \mathbb{R}^{n_\nu}$. The control problem is thus to minimize the *probability of an exit of the state of the power system from the critical set during a short horizon*. This problem belongs to the domain of stochastic control theory.

Fig. 2 illustrates the stochastic control problem. The vector of power supplies $p_s \in P^+$ determines the mean m and the standard deviation σ of any power line. The extremal probabilities that $(\theta_{i_k} - \theta_{j_k}) > +\pi/2$ and $(\theta_{i_k} - \theta_{j_k}) < -\pi/2$ are then to be minimized by a choice of the power supply vector.

The relation of the power supply vector to the probability. Note that a choice of a power supply vector from the domain of such vectors, determines both the mean and the standard deviation of the probability density function of the vector of phase-angle differences in power lines. The effects of control actuation on the mean and on the standard deviation are thus related. Because, by assumption, a power supply vector satisfies that the power supply equals the power demand, the goal of secondary frequency control is met. New in this problem is the distribution of the power supply vector over the nodes with power supply for reduction of the variance.

Variance reduction or the reduction of the standard deviation, has received much attention in control theory of stochastic systems. One such problem is control of motorway traffic where the road capacity plays a role of limiting the traffic flow, see [29].

3.2 The Control Objective Function

Definition 3.1 Consider the stochastic linearized power system of Section 2.8. Define the functions,

$$\begin{aligned} \forall k = (i_k, j_k) \in \mathbb{Z}_{n_{\mathcal{E}}}, \forall p_s \in P^+, \\ f_{as,k}(p_s) = |\theta_{s,i_k}(p_s) - \theta_{s,j_k}(p_s)| \\ = \arcsin(|(Ap_s + b)_k|), \end{aligned} \quad (15)$$

$$f_k(p_s) = f_{as,k}(p_s) + r \sigma_k(p_s) \in \mathbb{R}_+, \quad (16)$$

$$f(p_s) = \|(f_k(p_s))\|_{\infty} = \max_{k \in \mathbb{Z}_{n_{+1}}} f_k(p_s), \quad (17)$$

$$f_{as,k} : P^+ \rightarrow \mathbb{R}_+, f_{as} : P^+ \rightarrow \mathbb{R}^{n_{\mathcal{E}}},$$

$$f_k : P^+ \rightarrow \mathbb{R}_+, f : P^+ \rightarrow \mathbb{R}_+, r \in \mathbb{R}_{s+}.$$

Call f the control objective function and call $f(p_s)$ the value which represents the maximum over all power lines of an upper bound on the probability that the power flow in any power line is outside the critical set when the power supply vector is $p_s \in P^+$. The parameter $r \in \mathbb{R}_+$ is a parameter of the control objective function. The reader finds in Appendix .2.2 the formulas of the matrices A and b of $f_{as,k}(p_s)$.

For a particular decision vector $p_s \in P^+$ one computes the value $f(p_s)$ according to: (1) Solve the synchronous state equation (7) for the synchronous frequency vector $\theta_s \in (-\pi/2, +\pi/2)^{n_{\mathcal{E}}}$ and then compute $|m_k(p_s)|$ for all $k \in \mathcal{E}$. (2) Compute $F(\theta_s, 0)$ and the Jacobian matrix $J(\theta_s, 0)$. Use the matrices $(J(\theta_s, 0), K, C)$ and a reduction process, solve a Lyapunov equation, and then compute Q_y and $\sigma_k(p_s)$ for all $k \in \mathbb{Z}_{n_{\mathcal{E}}}$.

Problem 3.2 Control of the power flows to the critical subset. Solve the following optimization problem and determine a minimizer $p_s^* \in P^+$ and a value $a \in \mathbb{R}$.

$$\begin{aligned} a = f(p_s^*) &= \inf_{p_s \in P^+} f(p_s) \\ &= \inf_{p_s \in P^+} \max_{k=(i_k, j_k) \in \mathcal{E}} [|\theta_{s,i_k}(p_s) - \theta_{s,j_k}(p_s)| + r \sigma_k(p_s)]. \end{aligned}$$

If the value satisfies $a < \pi/2$ then there exists a decision vector $p_s \in P^+$ such that the probability that the state leaves the critical set during a short horizon according to the invariant probability distribution, is less than the value ϵ if $r = r_{\epsilon}$ is used in the cost function.

The control problem for a stochastic power system is now seen to be a problem of *control of the probability distribution of the power flows*. The input of the power supply vectors determines the probability distribution function of the power flows. The cost function is an upper bound on the probability that the power flows exit the critical subset, which probability is determined by the controlled probability distribution.

It is proven in a companion paper, [36], that the control objective function f defined above, is nondifferentiable and nonconvex. A minimizer of the function over the set of decision vectors exists and a procedure produces an approximation sequence which is proven to converge to a local minimizer. Duality of optimization theory is not applicable because the function is not convex.

For the record there follows a list of the main restrictions imposed on the control objective function.

1. From the probability of exiting the critical subset of the state set on a short horizon to the use of the invariant probability distribution of the power flows at a particular time during the short horizon.
2. From the probability of exiting the critical subset to an upper bound of this probability and to a subsequent approximation, see Section 2.10.

3.3 Comparison of Performance

Of interest to control of power system is the performance of a power system with control as proposed in this paper compared with a power system without control. In the existing literature, secondary frequency control has as control objectives for a short horizon: (1) that power supply equals power demand and (2) that an economic cost function is minimized. See for this control problem the papers, [8, 21, 40].

In this paper, the control objective of maintaining the phase-angle differences over power lines inside the critical set, is more important than the classical secondary frequency control with its emphasis on minimizing the economic cost.

Therefore, a comparison of the controlled system will be made with a particular form of a power system without control.

Define the *proportional control law* for the power supply vector by the following procedure for a short horizon. Consider the vector of maximal available power supply $p^{+,max}$ and the vector of power demands p^- which satisfy that $\sum_{i=1}^{n^+} p_i^{+,max} = p_{sum}^{+,max} \geq p_{sum}^- = \sum_{j=1}^{n^-} p_j^-$. Choose $p_{sum}^+ = p_{sum}^-$ hence power supply equals power demand. Define the fraction $s = p_{sum}^+ / p_{sum}^{+,max} \in (0, 1)$. Define then the power vector $p^+ \in \mathbb{R}^{n^+}$, $p_i^+ = s \times p_i^{+,max}$ for all $i \in \mathbb{Z}_{n^+}$. Then $\sum_{i=1}^{n^+} p_i^+ = p_{sum}^+ = p_{sum}^-$.

The comparison between without control and with control will then be focused on the values of,

$$\{(|\theta_{i_k} - \theta_{j_k}|, \sigma_k, f_k(p_s) = |\theta_{i_k} - \theta_{j_k}| + r\sigma_k), \forall k \in \mathcal{E}\}.$$

One expects that with control, the three values will decline with respect to without control. The results of this comparison are in the next section for the examples of a ring network and of a Manhattan grid.

4 The Performance of the Controlled Power System for Three Examples

Example 4.1 has been chosen because it has been used to illustrate the Braess paradox. Example 4.4 of a ring network has been chosen because such rings often occur in power networks. Example 4.5 of a Manhattan grid has been chosen because it was expected to be relatively stable.

The reader finds the details of the computations of the examples in a separate report, [34].

Example 4.1 An eight-node power network.

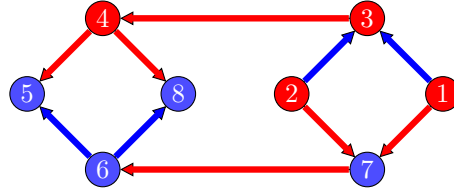


Figure 3: An eight-node academic example

This academic power network is borrowed from the paper [37]. It is often used to illustrate the Braess paradox. The network is displayed in Fig. 3, where the nodes which are colored red, 1, 2, 3, 4, provide power supply while nodes which are colored blue, 5, 6, 7, 8, have only power loads.

The parameters of the power system are the inertias, the damping coefficients, the standard deviations of the disturbances, the maximal power supplies and the power demands, and the line capacities. In a second part of the example for other cases, the parameter values are changed to different values. The results of the first part of the computations are displayed in Fig. 4. The columns of that column chart are ordered according to the values of $|\theta_i - \theta_j| + 2\sigma_{ij}$ in the decreasing order of magnitude.

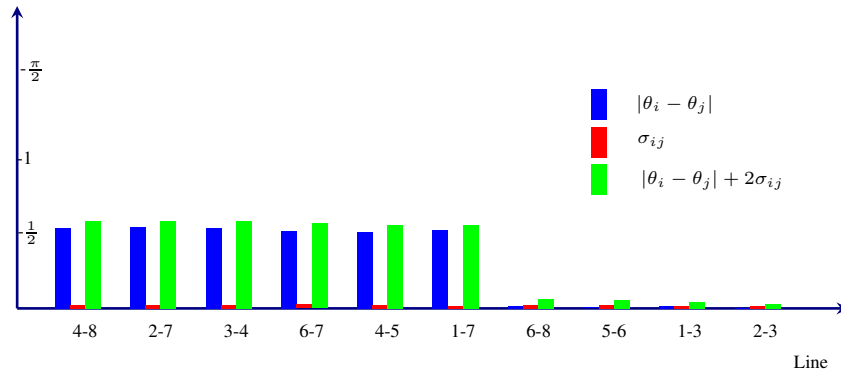


Figure 4: The outcomes of the Eight-node academic network

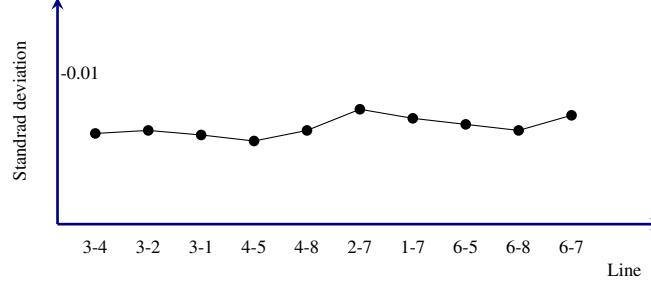


Figure 5: Propagation of a disturbance on node 3

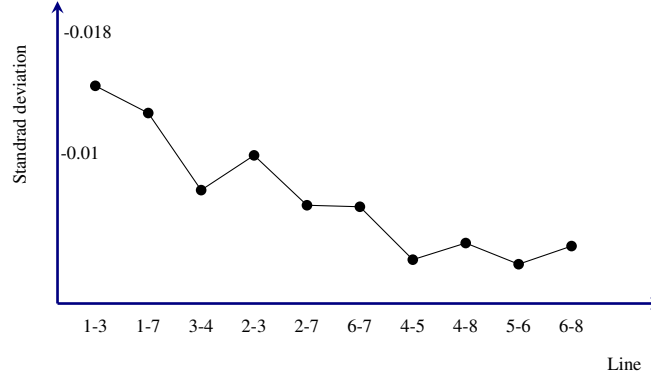


Figure 6: Propagation of a disturbance on node 1

The conclusions for this example are:

1. There are six lines with relatively high power flows which are colored red and four lines with relatively low power flows which are colored blue in Fig. 3.
2. For small standard deviations of disturbances compared to damping coefficients, the local minimizers are quite close to each other where-ever the initial state for the power supply vector is chosen.
3. When the values of the standard deviations of the disturbances increase then the local minimizers of the objective function can be easily distinguished.
4. It is very amazing that different minimizers have almost the same minimum values, see the Tables 3 and 4. The reason for this phenomenon is not yet clear to the authors.

Remark 4.2 A Braess paradox of Example 4.1. If one adds to the power network the line $(2, 4)$ between node 2 and node 4 or if one doubles only the capacity of line $(3, 4)$ then one expects that the value of the minimum will decrease. Yet, the value of the minimum increases, see the Tables 5 and 6 in contrast with Table 2. This is a paradoxical phenomenon, see the Braess paradox described in [10] and [30].

Remark 4.3 The spread of disturbance of Example 4.1. If there is only one disturbance at a particular node, one expects that the power lines, which are connected to that particular node, have larger fluctuations and power lines further away to have relatively lower fluctuations. However, the computation results show that this conjuncture is not always correct. Fig. 5 shows the results for the case when the standard deviation of the disturbance of node 3 is equal to 0.005 while those of the other nodes are 0; where line $3 - 4$, line $3 - 2$, line $3 - 1$ are lines which are connected to node 3 directly; line $4 - 5$, line $4 - 8$, line $2 - 7$ and line $1 - 7$ are one-edge away; line $6 - 5$, line $6 - 8$, line $6 - 7$ are two-edges away; one can see the magnitude of the standard deviation of the power flows go up and down slightly. Fig. 6 shows the results for the case when the standard deviation of the disturbance of node 1 is equal to 0.005 while those of the other nodes are 0; where line $1 - 3$, line $1 - 7$ directly connects to node 1; line $3 - 4$, line $2 - 3$, line $2 - 7$ and line $6 - 7$ are one-edge away; line $4 - 5$, line $4 - 8$, line $5 - 6$, line $6 - 8$ are two-edges away. One can see the magnitudes of the standard deviations of power flows decay with the distance. For the dynamics of phases, see [18].

Table 2: Example 4.1. The minimum value and the optimal power vector

Minimum	p_1	p_2	p_3	p_4
0.5779	12.0000	12.8293	13.0680	15.2443
	p_5	p_6	p_7	p_8
	-12	-12	-13	-13

Table 3: Example 4.1. Changes of the system parameters: standard deviations increased and the line capacity set to 35. Results of the minimum and the optimal power vector, from the initial power supply vector [12, 12, 12].

Minimum	p_1	p_2	p_3	p_4
1.2780	8.2883	7.7117	16.00	18.00
	p_5	p_6	p_7	p_8
	-12	-12	-13	-13

Table 4: Example 4.1. Changes of the system parameters: standard deviations increased and the line capacity set to 35. Results of the minimum and the optimal power vector, from the initial power supply vector [11, 11, 14].

Minimum	p_1	p_2	p_3	p_4
1.2768	1.9974	13.9974	15.9985	18.0067
	p_5	p_6	p_7	p_8
	-12	-12	-13	-13

Table 5: Example 4.1. Added is line 2 – 4. Results of the minimum value and the optimal power vector.

Minimum	p_1	p_2	p_3	p_4
0.6142	12.0001	14.0000	16.0000	11.1415
	p_5	p_6	p_7	p_8
	-12	-12	-13	-13

Table 6: Example 4.1. Change doubling the capacity of Line 3 – 4. Results of the minimum and the optimal power vector.

Minimum	p_1	p_2	p_3	p_4
0.6026	12.0000	14.0000	16.0000	11.1415
	p_5	p_6	p_7	p_8
	-12	-12	-13	-13

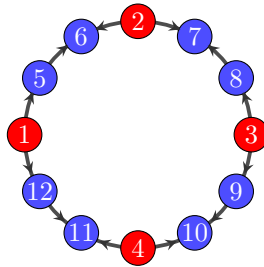


Figure 7: A ring network

Example 4.4 A ring network with twelve nodes. The power network shown in Fig. 7 consists of a ring with four red-colored nodes with power supply, 1, 2, 3 and 4, and eight blue-colored nodes with power demand. As for the Manhattan-grid network, the inertias and damping coefficients for nodes with power supply are relatively larger than those of power demand nodes. Due to the ring network structure, every neighborhood is connected to only two other neighborhoods, for example, the neighborhood (2, 6, 7) only connects to the neighborhood (1, 5, 12) and the neighborhood (3, 8, 9). The power network is inspired by [38], and the variance of a ring network structure is less than that of a tree-like structure for a rate $O(1/N)$ when they are subject to the same disturbances [35], where N is the number of nodes of these two network structures. Also, the authors in [23] introduced a method of curing dead

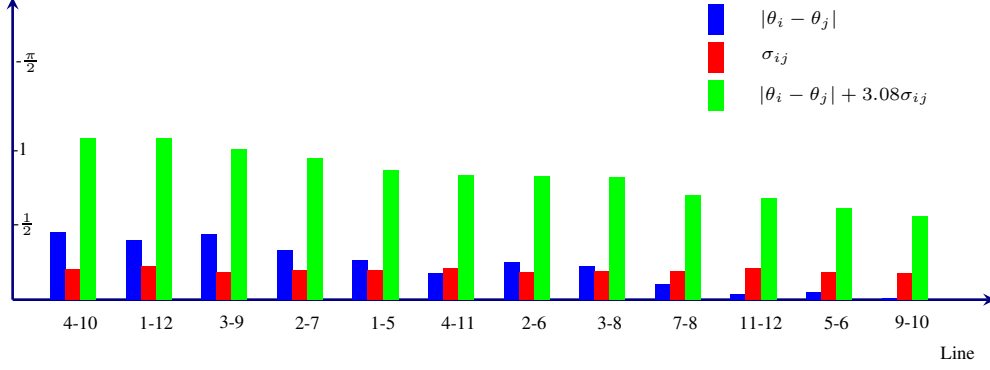


Figure 8: The outputs of the ring network starting from [20, 18, 25]

ends in power network by formulating a small ring structure. The parameter r of the objective function is chosen to be $r = 3.08$. The outcomes for a group of asymmetric network parameters starting from the power supply vector [20, 18, 25] are plotted in Fig. 8 and in Table 7 and Table 8.

Table 9 and Fig. 9 show the comparison of the performance of the power system without and with control as described in Subsection 3.3. For these computations, the standard deviations of the disturbances were higher than for the earlier computations. The table shows that, for the power lines with the highest values of $f_k(p_s)$, there is a significant reduction of the mean value $|\theta_{i_k} - \theta_{j_k}|$ and a small change of the standard deviation σ_k . Fig. 9 shows the effect of control on the probability density function of a power flow.

The conclusions of this example are:

1. For this specific ring network with these parameter values, two power supply vectors are quite close to each other, Tables 7 and 8.
2. There is a subset of two power lines of which both members have approximately the same values for the variable $|\theta_{i_k} - \theta_{j_k}| + r\sigma_{i_k, j_k}$.
3. In case the parameter values correspond to a symmetric network, then the power lines which connect neighborhoods, l_{5-6} , l_{7-8} , l_{9-10} , l_{11-12} in Fig. 7, have little power flow. The fluctuations of the power flows on those lines are not so high. For parameter values of an asymmetric network, there are relatively small power flows in those power lines.

Table 7: Example 4.4. The minimum value and optimal power vector starting from the power supply vector [20,18,25].

Minimum	p_1	p_2	p_3	p_4	p_5	p_6
1.0674	19.9368	20.0002	25.0001	19.0628	-6	-10
	p_7	p_8	p_9	p_{10}	p_{11}	p_{12}
	-8	-12	-17	-13	-7	-11

Table 8: Example 4.4. The minimum and optimal power vector starting from the power supply vector [23,19,24].

Minimum	p_1	p_2	p_3	p_4	p_5	p_6
1.0670	19.9749	20.0000	25.0000	19.0250	-6	-10
	p_7	p_8	p_9	p_{10}	p_{11}	p_{12}
	-8	-12	-17	-13	-7	-11

Example 4.5 A Manhattan-grid network.

The power network is displayed in Fig. 10. There are four red-colored nodes 1, 2, 3, and 4 with power supply with high inertias and damping coefficients which provide power to 21 blue-colored nodes with power demand with low virtual inertias and low damping coefficients. One may define for each node with only a power source, an imaginary neighborhood of nodes with only power demand which are largely supplied power by that particular power source.

Table 9: Example 4.4 The ring network. Comparison of performance without and with control.

Nodes		Control	$ \theta_{i_k} - \theta_{j_k} $	σ_k	$ \theta_{i_k} - \theta_{j_k} + r\sigma_k$
i_k	j_k				
4	10	without	0.5055	0.3076	1.4529
4	10	with	0.4041	0.3015	1.3328
1	12	without	0.4995	0.3344	1.5295
1	12	with	0.3302	0.3248	1.3307
3	9	without	0.3840	0.2730	1.2250
3	9	with	0.4615	0.2764	1.3127
2	7	without	0.3659	0.2952	1.2751
2	7	with	0.4615	0.2764	1.2727

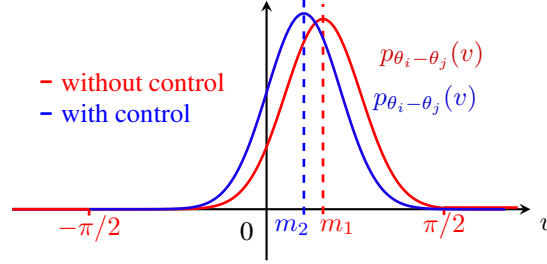


Figure 9: Example. Ring network, line 1-12, without and with control.

Then the power network is partitioned into several such neighborhoods and between such neighborhoods there is little power exchange. The Manhattan-grid power network has such an interpretation. The parameter r of the objective function is chosen to be 3.08, which leads to a probability of 99.8% of being inside the critical set. The computation results for the case of parameter values of an asymmetric power network, are shown in Fig. 11.

The reader finds in Table 10 the results for the comparison without and with control. The results are similar to those for the ring network and note that values of f_k are bounded away from $\pi/2 \approx 1.57$.

Table 10: Example 4.5. Comparison of performance without and with control.

Nodes		Control	$ \theta_{i_k} - \theta_{j_k} $	σ_k	$ \theta_{i_k} - \theta_{j_k} + r\sigma_k$
i_k	j_k				
1	7	without	0.5363	0.3149	1.5062
1	7	with	0.4990	0.3128	1.4625
4	23	without	0.5363	0.3128	1.4997
4	23	with	0.5046	0.3110	1.4625
3	16	without	0.5574	0.2589	1.3550
3	16	with	0.5932	0.2601	1.3943
2	14	without	0.5574	0.2590	1.3550
2	14	with	0.5932	0.2600	1.3941

The conclusions of this example are:

1. For this particular example the values of the standard deviations $\sigma_{i,j}$ are relatively high compared with those of $|\theta_i - \theta_j|$.
2. The reader may observe that for this particular power system, the power flowing from a node with power supply is larger than the power flow of any power line connected to that node, and, similarly, for the nodes with power demand. But no power outage is likely to occur, due to the tight interconnections of the Manhattan power grid, see Fig. 11. Thus, this particular power network has a very stable dynamic behavior due to the grid structure and the large number of power lines.
3. The optimization algorithm used is better than a method based on a grid of the feasible set of power supply vectors. This conclusion has been verified by a computation based on a grid of power supply vectors and by

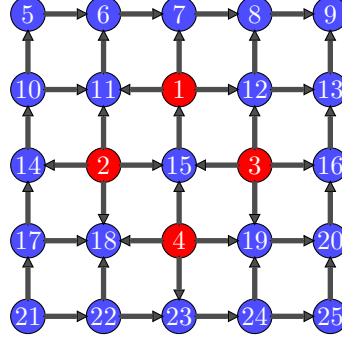


Figure 10: A Manhattan-grid like network

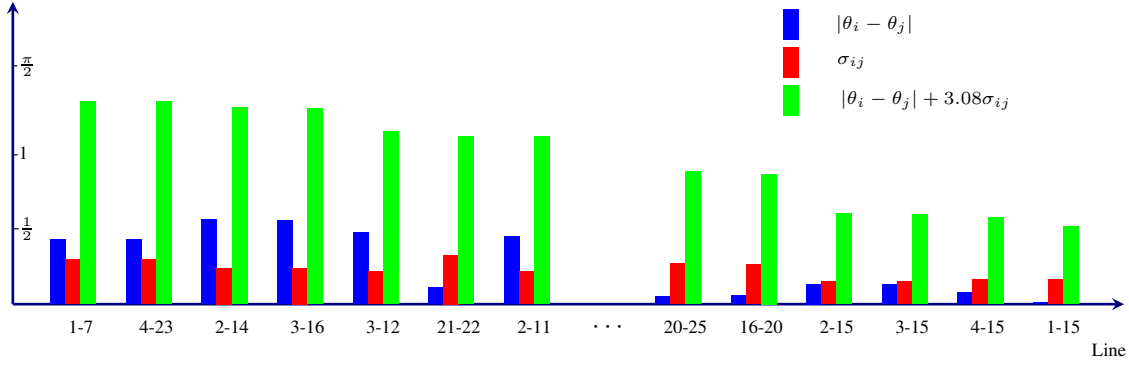


Figure 11: The outputs of the Manhattan-grid like network

computation of the control objective function at each grid point. The minimal values of the second method are in general larger than those of the steepest descent algorithm while the computation time is also larger.

4. A starting point for a vector of power supplies for the steepest descent algorithm may be taken as the sum of all nodes with power demands in a neighborhood of each node with power supply. The computational efficiency can be improved by such an initial choice.

4.1 Conclusions of All Three Examples

1. The descending order of the magnitude of the values of $f_k(p_s)$ of power lines of a stochastic power system, differ significantly from those of a deterministic power system, Figs. 4, 8, 11, where the columns are ordered in the descending order for the variable $f_k(p_s) = |\theta_{i_k} - \theta_{j_k}| + r\sigma_{(i_k, j_k)}$. The orders are different in case of the values of the absolute mean $|\theta_{i_k} - \theta_{j_k}|$ and of the standard deviation $\sigma_{(i_k, j_k)}$.
2. A byproduct of the computations is that it is directly clear which power lines have to be monitored by the power system operators during the short horizon for an exit from the critical set. For example, the first four power lines with the highest values in Fig. 11, are best monitored.
3. The reader sees from the length of the bars $f_k(p_s) = |\theta_i - \theta_j| + r\sigma_{ij}$, Figs. 4, 8, 11, that there is a subset of power lines of which all members have approximately the same values. This phenomenon is a property of the optimal solution for the considered examples.
4. The Manhattan grid network and the ring network are very stable due to the network structure.
5. The optimization algorithm used is better in terms of accuracy and efficiency than a computation method based on gridding the feasible set of power supply vectors into equal lengths.
6. The Braess' paradox also occurs in a stochastic power system.

5 Conclusions and Further Research

The emphasis of this paper on *control of the power flows* of a power system, is regarded as a useful focus for control of power systems. The power flows through all power lines of the power network are the main characteristic of a power system as a network. The concept of a critical subset of the state set and the probability that the state will exit the critical subset, are useful concepts for the analysis of a stochastic power system. The results for three examples show clearly that the performance as measured by the sum of the mean value and of a multiple of the standard deviation, differs from that of only the mean value or of only the standard deviation.

Needed for control theory of power systems and of stochastic system is further research on how the performance of the power system depends on: the graph of the power network and the distribution over the nodes of the power supplies and of the standard deviations of the disturbances. In addition, further research is needed on the performance of a power system with very low inertia in all nodes.

References

References

- [1] Aristotle Arapostathis, Shankar Sastry, and Pravin Varaiya. Global analysis of swing dynamics. *IEEE Transactions on Circuits and Systems*, 29(10):673–679, 1982.
- [2] S. Auer, F. Hellmann, M. Krause, and J. Kurths. Stability of synchrony against local intermittent fluctuations in tree-like power grids. *Chaos*, 27(12):127003, 2017.
- [3] John Baillieul and Cl Byrnes. Geometric critical point analysis of lossless power system models. *IEEE Transactions on Circuits and Systems*, 29(11):724–737, 1982.
- [4] H-D Chiang, Morris W Hirsch, and Felix F. Wu. Stability regions of nonlinear autonomous dynamical systems. *IEEE Transactions on Automatic Control*, 33(1):16–27, 1988.
- [5] H-D Chiang and James S Thorp. Stability regions of nonlinear dynamical systems: A constructive methodology. *IEEE Transactions on Automatic Control*, 34(12):1229–1241, 1989.
- [6] F. Dörfler and F. Bullo. Synchronization and transient stability in power networks and nonuniform Kuramoto oscillators. *SIAM J. Control Optim.*, 50(3):1616–1642, 2012.
- [7] F. Dörfler, M. Chertkov, and F. Bullo. Synchronization in complex oscillator networks and smart grids. *Proceedings of the National Academy of Sciences*, 110(6):2005–2010, 2013.
- [8] F. Dörfler and S. Grammatico. Gather-and-broadcast frequency control in power systems. *Automatica*, 79:296 – 305, 2017.
- [9] Mahyar Fazlyab, Florian Dörfler, and Victor M Preciado. Optimal network design for synchronization of coupled oscillators. *Automatica*, 84:181–189, 2017.
- [10] Marguerite Frank. The braess paradox. *Mathematical Programming*, 20(1):283–302, 1981.
- [11] I.I. Gikhman and A.V. Skorokhod. *Introduction to the theory of random processes*. W.B. Saunders Co., Philadelphia, 1969.
- [12] K. Glover and L.M. Silverman. Characterization of structural controllability. *IEEE Tr. Automatic Control*, 21:534–537, 1976.
- [13] Hauke Haehne, Katrin Schmietendorf, Samyak Tamrakar, Joachim Peinke, and Stefan Ketteman. Propagation of wind-power induced fluctuations in power grids. *Phys. Rev. E*, 99:050301, 2019.
- [14] Marija D Ilić and John Zaborszky. *Dynamics and control of large electric power systems*. Wiley New York, 2000.
- [15] Saber Jafarpour, Elizabeth Y. Huang, Kevin D. Smith, and Francesco Bullo. Flow and elastic networks on the n -torus: Geometry, analysis, and computation. *SIAM Review*, 64(1):59–104, 2022.
- [16] Samuel C. Johnson, Joshua D. Rhodes, and Michael E. Webber. Understanding the impact of non-synchronous wind and solar generation on grid stability and identifying mitigation pathways. *Applied Energy*, 262:114492, 2020.
- [17] I. Karatzas and S. Shreve. *Brownian motion and stochastic calculus*. Springer-Verlag, Berlin, 1988.
- [18] S. Kettemann. Delocalization of disturbances and the stability of AC electricity grids. *Phys. Rev. E*, 94:062311, 2016.

- [19] P. Kundur. *Power system stability and control*. McGraw-Hill, New York, 1994.
- [20] H. Kwakernaak and R. Sivan. *Linear optimal control systems*. Wiley-Interscience, New York, 1972.
- [21] N. Li, C. Zhao, and L. Chen. Connecting automatic generation control and economic dispatch from an optimization view. *IEEE Trans. Control Netw. Syst.*, 3(3):254–263, 2016.
- [22] Emma Marris. Upgrading the grid: Electricity grids must cope with rising demand and complexity in a changing world. emma marris explores the intricacies involved in controlling the power supply. *Nature*, 454(7204):570–574, 2008.
- [23] Peter J Menck, Jobst Heitzig, Jürgen Kurths, and Hans Joachim Schellnhuber. How dead ends undermine power grid stability. *Nature communications*, 5(1):3969, 2014.
- [24] Peter J Menck, Jobst Heitzig, Norbert Marwan, and Jürgen Kurths. How basin stability complements the linear-stability paradigm. *Nature physics*, 9(2):89–92, 2013.
- [25] Adilson E Motter, Seth A Myers, Marian Anghel, and Takashi Nishikawa. Spontaneous synchrony in power-grid networks. *Nature Physics*, 9(3):191–197, 2013.
- [26] K. Murota. *Matrices and matroids for systems analysis*. Springer-Verlag, Berlin, 2000.
- [27] B. K. Poolla, S. Bolognani, and F. Dörfler. Optimal placement of virtual inertia in power grids. *IEEE Trans. Autom. Control*, 62(12):6209–6220, 2017.
- [28] S. J. Skar. Stability of multi-machine power systems with nontrivial transfer conductances. *SIAM J. Appl. Math.*, 39(3):475–491, 1980.
- [29] Stef Smulders. Control of freeway traffic flow by variable speed signs. *Transportation Research Part B: Methodological*, 24(2):111–132, 1990.
- [30] Richard Steinberg and Willard I Zangwill. The prevalence of Braess’ paradox. *Transportation Science*, 17(3):301–318, 1983.
- [31] E. Tegling, B. Bamieh, and D. F. Gayme. The price of synchrony: Evaluating the resistive losses in synchronizing power networks. *IEEE Trans. Control Netw. Syst.*, 2(3):254–266, Sept 2015.
- [32] H.L. Trentelman, A.A. Stoorvogel, and M. Hautus. *Control theory for linear systems*. Springer, United Kingdom, 2001.
- [33] N Tsolas, Aristotle Arapostathis, and P Varaiya. A structure preserving energy function for power system transient stability analysis. *IEEE Transactions on Circuits and Systems*, 32(10):1041–1049, 1985.
- [34] Zhen Wang. Supplement of control of transient stability of a stochastic power system. Report, Delft University of Technology, Delft, The Netherlands, 2023.
- [35] Zhen Wang, Kaihua Xi, Aijie Cheng, Hai Xiang Lin, André C.M. Ran, Jan H. van Schuppen, and Chenghui Zhang. Synchronization of power systems under stochastic disturbances. *Automatica*, 151:110884, 2023.
- [36] Zhen Wang, Kaihua Xi, Aijie Cheng, Hai Xiang Lin, and Jan H. van Schuppen. Optimization of a nondifferentiable and nonconvex function for control of power systems. Report, Delft University of Technology, Delft, The Netherlands, 2023.
- [37] D. Witthaut and M. Timme. Braess’s paradox in oscillator networks, desynchronization and power outage. *New J. Phys.*, 14(8):083036, aug 2012.
- [38] K. Xi, J. L. A. Dubbeldam, and H. X. Lin. Synchronization of cyclic power grids: equilibria and stability of the synchronous state. *Chaos*, 27(1):013109, 2017.
- [39] K. Xi, H. X. Lin, C. Shen, and J. H. Van Schuppen. Multilevel power-imbalance allocation control for secondary frequency control of power systems. *IEEE Trans. Autom. Control*, 65(7):2913–2928, 2020.
- [40] Kaihua Xi, Johan L.A. Dubbeldam, Hai Xiang Lin, and Jan H. van Schuppen. Power-Imbalance Allocation Control of Power Systems-Secondary Frequency Control. *Automatica*, 92:72 – 85, 2018.
- [41] J. Zaborszky, G. Huang, T.C. Leung, and B.H. Zheng. Stability monitoring on the large electric power system. In *Proc. 24th Conference on Decision and Control*, pages 787–798, New York, 1985. IEEE Press.
- [42] J. Zaborszky, G. Huang, B. Zheng, and T. C. Leung. On the phase portrait of a class of large nonlinear dynamic systems such as the power system. *IEEE Trans. Autom. Control*, 33(1):4–15, jan 1988.
- [43] J. Zaborszky, K.W. Whang, K.V. Prasad, and I.N. Katz. Local feedback stabilization of large interconnected power system in emergencies. *Automatica*, 17:673–686, 1981.
- [44] X. Zhang, S. Hallerberg, M. Matthiae, D. Witthaut, and M. Timme. Fluctuation-induced distributed resonances in oscillatory networks. *Sci. Adv.*, 5(7):eaav1027, 2019.

- [45] X. Zhang, D. Witthaut, and M. Timme. Topological determinants of perturbation spreading in networks. *Phys. Rev. Lett.*, 125:218301, 2020.

Z. Wang

Zhen Wang was born in China, September 1995. He received his bachelor diploma in computational mathematics from Ningxia University, Yinchuan, China, in 2017. During 2015–2016, he attended the School of Mathematics of Jilin University. He is currently pursuing a Ph.D. degree at the School of Mathematics of Shandong University, in Jinan, Shandong Province, China. Since November 2021, he has been a visiting Ph.D. student at the Department of Applied Mathematics of Delft University of Technology in Delft, The Netherlands.

His research interests include computational mathematics, control theory, optimization, and stability analysis of power systems.

K. Xi

Kaihua Xi was awarded a Ph.D. degree by the Delft Institute of Applied Mathematics, Delft University of Technology, Delft, The Netherlands, in 2018. Currently, he is an associate professor at the School of Mathematics of Shandong University, Jinan, Shandong University, China.

His research interests include control, optimization and stability analysis of power systems, numerical algorithms of differential equations, and data assimilation of oil reservoir simulation.

A. Cheng

Aijie Cheng is Full Professor at the School of Mathematics, Shandong University, in Jinan, Shandong Province, China.

His research interests include numerical approximation of partial differential equations, and computational problems of science and engineering.

H. X. Lin

Hai Xiang Lin received a Ph.D. degree from Delft University of Technology. He is an associate professor at the Department of Mathematical Physics, Delft Institute of Applied Mathematics, Delft University of Technology. He is also a professor in Data Analytics for Environmental Modelling at the Institute of Environmental Sciences of Leiden University, on behalf of the R. Timman Foundation.

His research interests include high-performance computing, atmospheric and environmental modelling, data assimilation, big data, machine learning, simulation, and control of power systems. He has published more than 150 peer-reviewed Journal and international conference papers.

Dr. Lin is an Associate Editor of the journal *Algorithms and Computational Technology*, and an editorial board member of *Big Data Mining and Analytics*.

J. H. van Schuppen

Jan H. van Schuppen was born in Veenendaal, The Netherlands, October 1947. He was awarded an engineering diploma by Delft University of Technology in 1970 and a Ph.D. diploma in Electrical Engineering and Computer Science by the University of California at Berkeley, CA, USA in 1973.

As Professor Emeritus he is affiliated with the Department of Applied Mathematics of Delft University of Technology in Delft, The Netherlands since his retirement in October 2012 from the Centre of Mathematics and Computer Science (CWI). Since then he is active as a researcher with his consulting company Van Schuppen Control Research in Amsterdam, The Netherlands. His research interests include stochastic control and control of power systems.

Van Schuppen is a member of the IEEE Societies of Control Systems, Computers, and Information Theory, and of the Society for Industrial and Applied Mathematics (SIAM). He was an Associate-Editor-at-large of the *IEEE Transactions on Automatic Control*, a co-editor-in-Chief of the journal *Mathematics of Control, Signals, and Systems*, and was a Department Editor of *J. of Discrete-Event Dynamic Systems*.

The following appendices are included in the paper only for the review process. If the paper is accepted for publication then these appendices will be removed from the paper unless the Editor-in-Chief or the Associate Editor requests differently.

.1 Theory and Proofs of Section 2

.1.1 The Laplacian Matrix for a Complete Power Network

A complete network is defined as a network where every pair of distinct vertices is connected by a unique edge. In this case, the product $BWF(\theta_s)$ is equal to,

$$\begin{aligned} BWF_{i,j}(\theta_s) &= -L_{i,j} \cos(\theta_{s,i} - \theta_{s,j}), \\ &\quad \forall (i, j) \in \mathcal{E} \text{ with } i \neq j; \\ BWF_{k,k}(\theta_s) &= - \sum_{j=1, j \neq k}^{n_V} BWF_{k,j}(\theta_s), \quad \forall k \in \mathcal{E}. \end{aligned}$$

.1.2 Standard Deviation Strictly Positive

Proposition .1 (a) Consider the deterministic linear system from an input u to an output y ,

$$\begin{aligned} dx(t)/dt &= J(\theta_s, 0)x(t) + Ku(t), \quad x(0) = x_0, \\ y(t) &= Cx(t). \end{aligned}$$

Recall Assumption 2.1. Assume that the diagonal matrix K has strictly positive diagonal elements, hence, for all $k \in \mathcal{V}$, $K_{k,k} > 0$. A weaker condition is that (J_r, K_r) is a controllable pair. Then this system is a controllable system.

(b) For any power line $k \in \mathcal{E}$ and any fixed power supply vector $p_s \in P^+$, the standard deviation $\sigma_k(p_s)$ is strictly positive, $\sigma_k(p_s) = (Q_{y,(k,k)})^{1/2} > 0$.

Proof (a) (a.1) Consider the following Lyapunov equation for the variance of the phase-angle differences over the power lines,

$$\begin{aligned} 0 &= J(\theta_s, 0)Q_x + Q_x J(\theta_s, 0)^\top + KK^\top, \\ Q_y &= CQ_x C^\top, \\ J(\theta_s, 0) &= \begin{bmatrix} 0 & I_{n_V} \\ M^{-1}BWF(\theta_s) & -M^{-1}D \end{bmatrix}. \end{aligned}$$

Because the Laplacian matrix $BWF(\theta_s)$ has one zero eigenvalue, it is required to carry out a transformation and to truncate the system matrix $J(\theta_s, 0)$ to eliminate the zero eigenvalue, as described in [35]. Denote the combined transformation and truncation matrix as follows and then note the transformation of the Lyapunov equation,

$$\begin{aligned} n_{x_r} &= n_x - 1, \quad L \in \mathbb{R}^{n_{x_r} \times n_x}, \\ J_r &= LJ(\theta_s, 0)L^\top, \quad K_r = LK, \quad C_r = CL^\top, \\ Q_{x_r} &= LQ_x L^\top; \\ 0 &= J_r Q_{x_r} + Q_{x_r} J_r^\top + K_r K_r^\top; \quad \text{spec}(J_r) \subset \mathbb{C}^-; \\ Q_y &= CQ_x C^\top = CL^\top LQ_{x_r} L^\top LC^\top = C_r Q_{x_r} C_r^\top. \end{aligned}$$

(a.2) It will be argued that the tuple (J_r, K_r) is a controllable pair.

Define the undirected state graph $G_X = (V_X, E_X)$ with node set $V_X = \mathbb{Z}_{n_x}$ and edge set E_X by $(i, j) \in E$ if $J(\theta_s, 0)_{i,j} \neq 0$. Recall that $n_x = 2n_V$. Define the input-to-state graph as the undirected graph $G_{UX} = (V_{UX}, E_{UX})$ with $V_{UX} = \mathbb{Z}_{n_V} \times \mathbb{Z}_{n_V}$ and $(k, i) \in E_{UX}$ if $K_{i,k} \neq 0$.

Recall Section 2.2, that the graph of the power network is a connected set. It then follows from this assumption that, for any tuple $(i, j) \in E_X$, there exists a path from i to j .

Recall from the assumption of part (a) that for all $k \in \mathbb{Z}_{n_V}$, $K_{k,k} > 0$. It then follows that, for any $i + n_V \in \mathbb{Z}_{n_x}$, there exists a $k = i \in \mathbb{Z}_{n_V}$ and a path from u_k to x_i . Because the differential equation of the power system includes

the equation that, for all $i \in \mathbb{Z}_{n_V}$, $d\theta_i(t)/dt = \omega_i(t)$, there exists for each such i an integer $k = i \in \mathbb{Z}_{n_V}$ and a path from u_k to x_i via $x_{i+n_V} = \omega_i$.

(a.3) From Theorem [26, Thm. 6.4.2] follows that the time-invariant linear system is controllable if and only if (1) there exists a set of mutually disjoint cycles and stems such that all nodes of V_X are covered; and (2) for every node of a state there exists a path from an input to that state. This is also proven in [12]. That condition (1) holds follows from the assumption that the power network is a connected set. It was proven above that condition (2) holds. Thus the tuple $(J(\theta_s, 0), K)$ is a controllable pair. The same conclusion holds for the tuple (J_r, K_r) because the deletion of a component with a zero eigenvalue for all concerned matrices does not affect the controlability property, except that it now applies to the truncated linear system.

(b) It follows from $\text{spec}(J_r) \subset \mathbb{C}^-$, (J_r, K_r) a controllable pair, and [32, Thm. 3.28] for the direction that (1) and (2) imply (3), that $Q_{x_r} \succ 0$, hence is strictly positive-definite and symmetric. Denote by $C(k, \text{row})$ the k -th row of the matrix C , the first part of which equals the k -th column of the matrix B . It then follows from the definition of the matrix B that there are two nonzero elements of $C(k, \text{row})$. This result and $Q_{x_r} \succ 0$ imply that,

$$\begin{aligned} \forall k \in \mathbb{Z}_{n_E}, \sigma_k &= (Q_{y, (k, k)})^{1/2} \\ &= (C(k, \text{row})Q_{x_r}C(k, \text{row})^\top)^{1/2} > 0. \end{aligned}$$

□

Denote respectively the probability density function and the probability distribution function of $G(0, 1)$ by $p_G : \mathbb{R} \rightarrow \mathbb{R}_+$ and $f_G : \mathbb{R} \rightarrow \mathbb{R}_+$. Because p_G is symmetric when mirrored at 0, thus for all $v \in \mathbb{R}$, $p_G(v) = p_G(-v)$, it follows that, for all $r \in \mathbb{R}$, $1 - f_G(r) = f_G(-r)$.

1.3 Proof of Proposition 2.10

Proof (a) For all $k \in \mathbb{Z}_{n_E}$, and for all $p_s \in P^+$, the probability that the power flow of the k -th power line goes into the unstable region according to the invariant probability distribution of the power line flow, is equal to,

$$\begin{aligned} p_{\text{outc}, k}(p_s) &= P(\{\omega \in \Omega \mid \theta_{i_k}(\omega, t) - \theta_{j_k}(\omega, t) < -\pi/2\}) + \\ &+ P(\{\omega \in \Omega \mid \theta_{i_k}(\omega, t) - \theta_{j_k}(\omega, t) > +\pi/2\}) \\ &= P\left(\left\{\omega \in \Omega \mid \frac{(\theta_{i_k}(\omega, t) - \theta_{j_k}(\omega, t)) - m_k(p_s)}{\sigma_k(p_s)} \right. \right. \\ &\quad \left. \left. < \frac{-\pi/2 - m_k(p_s)}{\sigma_k(p_s)} \right\}\right) + P \dots \\ &= f_{G(0,1)}(r_{a,k}(p_s)) + [1 - f_{G(0,1)}(r_{b,k}(p_s))] \\ &= f_{G(0,1)}(r_{a,k}(p_s)) + f_{G(0,1)}(-r_{b,k}(p_s)), \\ r_{a,k}(p_s) &= \frac{-\pi/2 - m_k(p_s)}{\sigma_k(p_s)}, \\ -r_{b,k}(p_s) &= \frac{-\pi/2 + m_k(p_s)}{\sigma_k(p_s)}, \\ r_{a,b,k}(p_s) &= \frac{-\pi/2 - |m_k(p_s)|}{\sigma_k(p_s)}, \\ m_k(p_s) &\in (-\pi/2, +\pi/2) \Rightarrow \\ r_{a,k}(p_s) &< 0, \quad -r_{b,k}(p_s) < 0. \end{aligned}$$

Because the probability distribution function f_G is strictly monotone, the definition of $r_{a,b,k}$ and the monotonicity of f_G imply the equality of $f_G(r_{a,b,k}(p_s))$.

(b) By definition $f_{G(0,1)}(r_{\epsilon/2}) \leq \epsilon/2$, for example, if $\epsilon/2 = 10^{-3}$ then $r_{\epsilon/2} = -3.08$. Assume that $r_{a,b,k}(p_s) \leq r_{\epsilon/2}$. Then,

$$\begin{aligned} r_{a,k}(p_s) &\leq \max\{r_{a,k}(p_s), -r_{b,k}(p_s)\} \\ &= r_{a,b,k}(p_s) \leq r_{\epsilon/2}, \text{ and similarly,} \\ -r_{b,k}(p_s) &\leq \max\{r_{a,k}(p_s), -r_{b,k}(p_s)\} \\ &= r_{a,b,k}(p_s) \leq r_{\epsilon/2}, \Rightarrow \\ p_{outc,k}(p_s) &= f_{G(0,1)}(r_{a,k}(p_s)) + f_{G(0,1)}(-r_{b,k}(p_s)) \\ &\leq \epsilon. \end{aligned}$$

The existence of $p_s^* \in P^+$ follows from a result of [36] and the lower bound from the implications,

$$\begin{aligned} f_d^* &\leq \pi/2 \Rightarrow \forall k \in \mathbb{Z}_{n\epsilon}, \\ r_{a,b,k}(p_s^*) &= \frac{-\pi/2 + |m_k(p_s^*)|}{\sigma_k(p_s^*)} \leq \frac{-\pi/2 + f_d^*}{\sigma_k(p_s^*)} + r_\epsilon \leq r_\epsilon \\ p_{outc}(p_s^*) &\leq 2\epsilon. \end{aligned}$$

□

.2 Theory of Section III

.2.1 Formulas of A_1, b_1, b_2 of Def. 3.1

Table 11: Formulas of computation of the matrices A and b of Def. 3.1.

$$\begin{aligned} B^\top (BW B^\top)^\dagger p_{sp} &= B^\top U^\top \Lambda^\dagger U p_{sp} \\ &= B^\top U^\top \Lambda^\dagger U \left[p_1, \dots, p_{n+1}, p_{sum}^- - p_1 - \dots - p_{n+1}, -p_{n+1}^{-,max}, \dots, -p_n^{-,max} \right]^\top \\ &= B^\top U^\top \Lambda^\dagger \left(p_1 (U(1, col) - U(n^+, col)) + \dots + p_{n+1} (U(n^+ - 1, col) - U(n^+, col)) \right. \\ &\quad \left. + p_{sum}^- U(n^+, col) - p_{n+1}^{-,max} U(n^+ + 1, col) - \dots - p_n^{-,max} U(n, col) \right) \\ &= B^\top U^\top \Lambda^\dagger \left(p_1 (U(1, col) - U(n^+, col)) + \dots + p_{n+1} (U(n^+ - 1, col) - U(n^+, col)) + \right. \\ &\quad \left. + p_{n+1}^{-,max} (U(n^+, col) - U(n^+ + 1, col)) + \dots + p_n^{-,max} (U(n^+, col) - U(n, col)) \right) \\ &\text{define} \\ p_s &= [p_1, p_2, \dots, p_{n+1}]^\top, \\ -p_d &= [-p_{n+1}^{-,max}, -p_{n+2}^{-,max}, \dots, -p_n^{-,max}]^\top; \\ &= B^\top U^\top \Lambda^\dagger [U(1, col) - U(n^+, col), \dots, U(n^+ - 1, col) - U(n^+, col)] p_s + \\ &\quad + B^\top U^\top \Lambda^\dagger [U(n^+ + 1, col) - U(n^+, col), \dots, U(n, col) - U(n^+, col)] p_d \\ &\text{define} \\ A &= B^\top U^\top \Lambda^\dagger [U(1, col) - U(n^+, col), \dots, U(n^+ - 1, col) - U(n^+, col)], \\ b &= B^\top U^\top \Lambda^\dagger [U(n^+ + 1, col) - U(n^+, col), \dots, U(n, col) - U(n^+, col)] p_d; \\ &= A p_s + b. \end{aligned}$$

$$\begin{aligned}
A_1 &= \begin{bmatrix} 1 & 0 & 0 & \cdots & 0 \\ 1 & 1 & 0 & \cdots & 0 \\ 1 & 1 & 1 & \cdots & 0 \\ \vdots & \vdots & \vdots & \ddots & \vdots \\ 1 & 1 & 1 & \cdots & 1 \end{bmatrix} \in \mathbb{R}^{(n^+-1) \times (n^+-1)}, \\
b_1 &= \begin{bmatrix} p_{sum}^- - p_{n^+}^{+,max} - \cdots - p_2^{+,max} \\ p_{sum}^- - p_{n^+}^{+,max} - \cdots - p_3^{+,max} \\ p_{sum}^- - p_{n^+}^{+,max} - \cdots - p_4^{+,max} \\ \vdots \\ p_{sum}^- - p_{n^+}^{+,max} \end{bmatrix} \in \mathbb{R}^{(n^+-1) \times 1}, \\
b_2 &= \begin{bmatrix} p_1^{+,max} & p_2^{+,max} & p_3^{+,max} & \cdots & p_{n^+-1}^{+,max} \end{bmatrix}^\top \\
&\in \mathbb{R}^{(n^+-1) \times 1}.
\end{aligned}$$

.2.2 Computation of the Matrices A and b of Def. 3.1

By Theorem 2.2 and [9, Prop. 1], the sin values of phase-angle differences satisfy $\sin(B^\top \theta^*) = B^\top (BWB^\top)^\dagger p_{sp}$ and then we transform the matrix $(BWB^\top)^\dagger$ into a diagonal matrix:

$$\hat{U}^\top (BWB^\top) \hat{U} = \Lambda \Rightarrow (BWB^\top)^\dagger = \hat{U} \Lambda^\dagger \hat{U}^\top.$$

Define $U = \hat{U}^\top$, which makes $(BWB^\top)^\dagger = U^\top \Lambda^\dagger U$, See Table 11 for the formulas.

.2.3 Two Alternative Optimization Criteria

There are two alternative optimization criteria which the authors have considered but decided not to use. An explanation follows.

The first alternative criterion is the infimum over all power supply vectors of the probability that the first exit time τ_1 from the domain of attraction is less than the duration of the short horizon t_p ,

$$\begin{aligned}
&\inf_{p^+ \in P^+} P(\{\omega \in \Omega \mid \tau_1(\omega) \leq t_p\}), \\
&\tau_1 : \Omega \rightarrow \mathbb{R}_+ \cup \{+\infty\}, \\
&\tau_1(\omega) \\
&= \begin{cases} \inf_{t \in [0, +\infty)} \\ \left\{ \max_{k \in \mathbb{Z}_{n_\mathcal{E}}} |\theta_{i_k}(\omega, t) - \theta_{j_k}(\omega, t)| > \pi/2 \right\}, \\ \text{if such a time exists,} \\ +\infty, \text{ else.} \end{cases}
\end{aligned}$$

This criterion is the most realistic one. However, the difficulty with this criterion is that it is difficult to compute or to numerically approximate. It is computationally expensive to compute all type-one states and then to compute one such state with the lowest value for the energy function. A type-one steady state is a synchronous state such that the linearized system has a Jacobian matrix with only one eigenvalue with a strictly positive real part. This requires the computation of the *Jacobian matrix*. In addition, estimating the probability distribution of the first exit time based on simulations is expensive because the exit is a rare event requiring many simulations. The technique of importance sampling can be used for this computation but that still requires a considerable computational effort.

The second alternative criterion is the infimum over all power supply vectors of the probability that the maximum of the phase-angle difference is less than $\pi/2$, where the probability distribution is the invariant Gaussian probability distribution of the output of the stochastic system. In terms of mathematical notation, this criterion equals,

$$\inf_{p^+ \in P^+} P \left(\left\{ \omega \in \Omega \mid \max_{k \in \mathbb{Z}_{n_\mathcal{E}}} \sup_{t \in [0, t_p)} |\theta_{i_k}(\omega, t) - \theta_{j_k}(\omega, t)| > \pi/2 \right\} \right).$$

In this case the invariant probability distribution is used rather than the probability distribution of the exit time. The value of this criterion for a particular supply vector is also difficult to compute because there are no tables for the maximum of a finite set of correlated Gaussian random variables. The tail of the probability distribution is fatter than that of the Gaussian distribution so that is not simple to compute an upper bound on the probability.

For these reasons, the authors prefer the cost criterion of Def. 3.1.

Supplement of 'Control of the Power Flows of a Stochastic Power System'

Zhen Wang *

November 29, 2023

1 Introduction

The purpose for this supplement is to provide the direct outcomes of the descent procedure for the three examples investigated in the main body of the paper. The parameters of specific power systems can be used for computations and are listed so as to allow reproduction. From these results, the readers may learn the descent procedure. Furthermore, the figures in the manuscript are plotted based on the particular tables listed in this supplement. Fig. 4 is based on Table 5; Fig. 5 is based on Table 13; Fig. 6 is based on Table 15; Fig. 8 is based on Table 28; and Fig. 11 is based on Table 39.

Paper organization Section 2 deals with the eight-node academic example. Its original parameters and original outcomes are listed. Afterwards, some of the parameters of this particular power network are changed in order to investigate their influence on the outcomes. Section 3 deals with a Manhattan-grid network. Since it is a symmetric network-structure, we first make every kind of parameter symmetric to see what will the outcomes look like. Next, we make the power demand vector asymmetric and similarly the disturbance vector, to compare the results. Since this network is large, it will cost more time to compute the minimizer than small networks, hence we do not investigate the influence on the outcomes by changing the network parameters of this power system. Section 4 deals with a twelve-node ring network, its network structure is also symmetric, like Manhattan-grid network, we first make every kind of parameter symmetric to investigate the outcomes. Secondly, every kind of parameter is changed in order to see its influence on the outcomes. What's more, Sections 3 and 4 also compare the computation results with the performance of a power system without control.

2 Tables of the Eight-Node Academic Example

The picture of eight-node academic network is displayed in Fig. 1 where the nodes 1, 2, 3, 4 have power supply and the other nodes have power demand. Tables 1 and 2 show the parameters of this eight-node academic power system while Table 3 displays the maximum power supply and demand of each power node, one can check these specified values satisfy our assumption 2.4.

Table 4 shows the minimum of control objective function and the optimal power supply vector computed by the descent procedure. The computation has been additionally been evaluated by discretizing the set of three power supply vectors for each dimension into a grid with 150 steps. The minimum value computed by this grid method is 0.5782 which is slightly larger than the minimum computed by the descent procedure. Table 5 shows the absolute value of mean of the phase-angle difference of each power line: $|\theta_i - \theta_j|$, the standard deviation of the phase-angle difference σ_{ij} , the component of our object function $|\theta_i - \theta_j| + 2\sigma_{ij}$ and the power flow $l_{ij} \sin(|\theta_i - \theta_j| + 2\sigma_{ij})$ on each power line and

*Zhen Wang is with the School of Mathematics, Shandong University, Jinan, 250100, Shandong Province, China and is visiting the Dept. of Applied Mathematics, Delft University of Technology, Delft, The Netherlands from November 2021 till February 2024 (email: wangzhen17@mail.sdu.edu.cn). Zhen Wang is grateful to the China Scholarship Council (No. 202106220104) for financial support for his stay at Delft University of Technology in Delft, The Netherlands.

the rows of this table are sorted by $|\theta_i - \theta_j| + 2\sigma_{ij}$ in descending order. In this example, the parameter r is chosen as 2, which leads to a trust probability of 95.45%.

Tables 6 and 7 show the outcomes after adding line 2 – 4 while Tables 8 and 9 present the consequences after doubling the capacity of line 3 – 4. Recent publications have already investigated the propagation of disturbance based on their experimental findings or analytical formulas. We have also investigated this issue in this report. We illustrate the effect of the disturbances by putting a disturbance only at node 3 and the outcomes are displayed in Tables 10 and 11, where one can see that the fluctuations drop tremendously. By addressing only one node with a disturbance and we use the standard deviation of phase-angle difference σ_{ij} to quantify the fluctuation of transmission line $i - j$. Tables 12 and 13 demonstrate the outcomes if there is only a disturbance at node 3. As a comparison group, we show the outcomes if there is only a disturbance at node 1 in Tables 14 and 15. Up to this point, all the results were computed by the descent procedure from the initial power supply vector [12, 12, 12].

The performance of the controlled power system as specified in Tables 14 and 15, is now contrasted with the computational results obtained from the initial power supply vector [11, 11, 14] in Tables 16 and 17 and we can get that the minimizer in Table 14 differs a little but not so much compared with the minimizer in Table 16. The reason might be the strength of the disturbance is too small. Hence, we need to increase the strength of the disturbance to see its impact on the convexity property of the control objective function. For this purpose, we only show the minimum value of the control objective function and the optimal power vector and we do not show the outcomes of absolute value of mean of phase-angle differences, the standard deviations, etc. We first enlarge the strength of disturbances to be 10 times the earlier values, the outcomes are shown in Tables 18 and 19 starting from the power supply vectors [12, 12, 12] and [11, 11, 14], separately. One can see that the minimizers don't differ so much. Under this specification of disturbances, we enlarge the strength of disturbances once more, but only at some nodes and enlarge the line capacity to 35, the outcomes are shown in Table 20 starting from the power supply vector [12, 12, 12] and Table 21 starting from the power supply vector [11, 11, 14]. Here, we can see the minimizers differ more obviously. Finally, we increase all the standard deviations of the disturbances and the outcomes are displayed in Table 20 starting from the power supply vector [12, 12, 12] and Table 21 starting from the power supply vectors [11, 11, 14]. One can see there are two different minimizers. Furthermore, readers can also conclude that the minimum values are very close to each other even if the minimizers differ a lot from these six tables. Moreover, the largest value and second largest value of vector $|\theta_i - \theta_j| + 2\sigma$ differ very little and this may be due to the optimal solution.

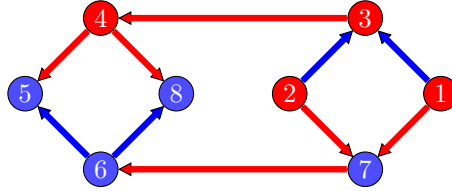


Figure 1: The eight-node academic example

Table 1: The network parameters:

i , node	1	2	3	4	5	6	7	8
m_i , inertia	0.1	0.2	0.3	0.4	0.5	0.6	0.7	0.8
d_i , damping	0.00123	0.00127	0.00122	0.00128	0.00121	0.00129	0.00118	0.00132
$K_2(i, i)$, disturbance	0.003	0.004	0.005	0.006	0.007	0.008	0.009	0.01

Table 2: Line capacities

Line	1-3	1-7	2-3	2-7	3-4	4-5	4-8	5-6	6-7	6-8	2-4
Capacities	25	25	25	25	25 or 50	25	25	25	25	25	0 or 25

Table 3: Power supply and power demand

Power	$p_1^{+,max}$	$p_2^{+,max}$	$p_3^{+,max}$	$p_4^{+,max}$	$p_5^{-,max}$	$p_6^{-,max}$	$p_7^{-,max}$	$p_8^{-,max}$
	12	14	16	18	12	12	13	13

Table 4: The minimum and optimal power vector start from the power supply vector [12, 12, 12]

Minimum	p_1	p_2	p_3	p_4	p_5	p_6	p_7	p_8
0.5779	12.0000	12.8288	13.0688	12.1024	-12	-12	-13	-13

Table 5: Phase-angle differences and other outputs start from the power supply vector [12, 12, 12]

i	j	$ \theta_i - \theta_j $	σ_{ij}	$ \theta_i - \theta_j + 2\sigma_{ij}$	$l_{ij} \sin(\theta_i - \theta_j + 2\sigma_{ij})$
3	4	0.5326	0.0227	0.5779	13.6571
4	8	0.5305	0.0237	0.5779	13.6571
2	7	0.5379	0.0200	0.5779	13.6570
6	7	0.5099	0.0258	0.5615	13.3124
4	5	0.5074	0.0231	0.5536	13.1448
1	7	0.5187	0.0165	0.5517	13.1042
6	8	0.0141	0.0242	0.0625	1.5620
5	6	0.0059	0.0239	0.0538	1.3436
1	3	0.0158	0.0140	0.0439	1.0960
2	3	8.0340e-04	0.0150	0.0308	0.7688

Table 6: Adding line 2–4, the minimum value and optimal power vector start from the power supply vector [12, 12, 12]

Minimum	p_1	p_2	p_3	p_4	p_5	p_6	p_7	p_8
0.6142	12.0001	14.0000	16.0000	7.9999	-12	-12	-13	-13

Table 7: Adding line 2–4, the phase-angle differences and other outputs start from the power supply vector [12, 12, 12]

i	j	$ \theta_i - \theta_j $	σ_{ij}	$ \theta_i - \theta_j + 2\sigma_{ij}$	$l_{ij} \sin(\theta_i - \theta_j + 2\sigma_{ij})$
4	8	0.5670	0.0236	0.6142	14.4068
4	5	0.5435	0.0234	0.5903	13.9151
1	7	0.5536	0.0173	0.5881	13.8690
3	4	0.4588	0.0180	0.4948	11.8705
6	7	0.4398	0.0257	0.4912	11.7925
2	7	0.4334	0.0182	0.4699	11.3203
2	4	0.2957	0.0151	0.3260	8.0057
2	3	0.1520	0.0138	0.1796	4.4657
5	6	0.0372	0.0239	0.0850	2.1231
1	3	0.0457	0.0142	0.0742	1.8522
6	8	0.0171	0.0243	0.0658	1.6438

Table 8: Doubling capacity of line 3–4, the minimum and optimal power vector start from the power supply vector [12, 12, 12]

Minimum	p_1	p_2	p_3	p_4	p_5	p_6	p_7	p_8
0.6026	12.0000	14.0000	16.0000	7.9999	-12	-12	-13	-13

Table 9: Doubling capacity of line 3 – 4, the phase-angle differences and other outputs start from the power supply vector [12, 12, 12]

i	j	$ \theta_i - \theta_j $	σ_{ij}	$ \theta_i - \theta_j + 2\sigma_{ij}$	$l_{ij} \sin(\theta_i - \theta_j + 2\sigma_{ij})$
4	8	0.5552	0.0237	0.6026	14.1702
4	5	0.5319	0.0234	0.5787	13.6734
2	7	0.5269	0.0187	0.5643	13.3716
6	7	0.4620	0.0263	0.5146	12.3039
1	7	0.4812	0.0163	0.5137	12.2856
3	4	0.3652	0.0137	0.3925	19.1254
2	3	0.0572	0.0161	0.0894	2.2315
5	6	0.0271	0.0245	0.0762	1.9042
6	8	0.0071	0.0246	0.0563	1.4063
1	3	0.0171	0.0148	0.0467	1.1673

Table 10: Doubling the capacity of line 3 – 4, there is only a disturbance at node 3 with strength 0.005, the minimum value and optimal power vector start from the power supply vector [12, 12, 12]

Minimum	p_1	p_2	p_3	p_4	p_5	p_6	p_7	p_8
0.5666	12.0001	14.0000	16.0000	7.9999	-12	-12	-13	-13

Table 11: Doubling the capacity of line 3 – 4, there is only a disturbance on node 3 with the strength 0.005, the phase-angle differences and other outputs start from the power supply vector [12, 12, 12]

i	j	$ \theta_i - \theta_j $	σ_{ij}	$ \theta_i - \theta_j + 2\sigma_{ij}$	$l_{ij} \sin(\theta_i - \theta_j + 2\sigma_{ij})$
4	8	0.5552	0.0057	0.5666	13.4192
4	5	0.5319	0.0056	0.5431	12.9197
2	7	0.5269	0.0057	0.5382	12.8149
1	7	0.4812	0.0073	0.4959	11.8952
6	7	0.4620	0.0052	0.4723	11.3733
3	4	0.3652	0.0045	0.3741	18.2729
2	3	0.0572	0.0049	0.0669	1.6710
5	6	0.0271	0.0058	0.0388	0.9698
1	3	0.0171	0.0067	0.0306	0.7658
6	8	0.0071	0.0055	0.0182	0.4545

Table 12: There is only a disturbance with a strength 0.005 at node 3 , the minimum value and optimal power vector start from the power supply vector [12, 12, 12]

Minimum	p_1	p_2	p_3	p_4	p_5	p_6	p_7	p_8
0.5438	12.0000	12.2427	13.5367	12.2207	-12	-12	-13	-13

Table 13: There is only a disturbance with a strength 0.005 at node 3 , the phase-angle differences and other output start from power the supply vector [12, 12, 12]

i	j	$ \theta_i - \theta_j $	σ_{ij}	$ \theta_i - \theta_j + 2\sigma_{ij}$	$l_{ij} \sin(\theta_i - \theta_j + 2\sigma_{ij})$
4	8	0.5329	0.0055	0.5438	12.9358
2	7	0.5287	0.0076	0.5438	12.9358
3	4	0.5319	0.0060	0.5438	12.9355
1	7	0.5231	0.0070	0.5370	12.7898
4	5	0.5098	0.0052	0.5202	12.4266
6	7	0.5052	0.0072	0.5197	12.4145
1	3	0.0196	0.0059	0.0313	0.7822
2	3	0.0147	0.0062	0.0271	0.6778
6	8	0.0120	0.0062	0.0244	0.6096
5	6	0.0080	0.0066	0.0212	0.5301

Table 14: There is only a disturbance with a strength 0.005 at node 1 , the minimum value and optimal power vector start from the power supply vector [12, 12, 12]

Minimum	p_1	p_2	p_3	p_4	p_5	p_6	p_7	p_8
0.5429	11.9827	12.5107	12.7931	12.7135	-12	-12	-13	-13

Table 15: There is only a disturbance with a strength 0.005 at node 1 , the phase-angle differences and other output start from the power supply vector [12, 12, 12]

i	j	$ \theta_i - \theta_j $	σ_{ij}	$ \theta_i - \theta_j + 2\sigma_{ij}$	$l_{ij} \sin(\theta_i - \theta_j + 2\sigma_{ij})$
2	7	0.5299	0.0065	0.5429	12.9161
4	8	0.5350	0.0040	0.5429	12.9161
1	7	0.5177	0.0126	0.5429	12.9160
3	4	0.5134	0.0075	0.5284	12.6045
4	5	0.5119	0.0029	0.5177	12.3727
6	7	0.5010	0.0064	0.5137	12.2861
1	3	0.0156	0.0144	0.0443	1.1082
2	3	0.0050	0.0098	0.0246	0.6149
6	8	0.0102	0.0038	0.0177	0.4425
5	6	0.0098	0.0026	0.0150	0.3745

Table 16: There is only a disturbance with a strength 0.005 at node 1 , the minimum value and optimal power vector start from the power supply vector [11, 11, 14]

Minimum	p_1	p_2	p_3	p_4	p_5	p_6	p_7	p_8
0.5429	11.7953	12.3226	13.3546	12.5275	-12	-12	-13	-13

Table 17: There is only a disturbance with a strength 0.005 at node 1 , phase-angle differences and other output start from the power supply vector [11, 11, 14]

i	j	$ \theta_i - \theta_j $	σ_{ij}	$ \theta_i - \theta_j + 2\sigma_{ij}$	$l_{ij} \sin(\theta_i - \theta_j + 2\sigma_{ij})$
2	7	0.5299	0.0065	0.5429	12.9160
1	7	0.5177	0.0126	0.5429	12.9160
4	8	0.5350	0.0040	0.5429	12.9159
3	4	0.5220	0.0075	0.5370	12.7894
4	5	0.5119	0.0029	0.5177	12.3726
6	7	0.5010	0.0064	0.5137	12.2859
1	3	0.0231	0.0144	0.0518	1.2956
2	3	0.0125	0.0098	0.0321	0.8023
6	8	0.0102	0.0038	0.0177	0.4423
5	6	0.0098	0.0026	0.0150	0.3748

Table 18: Increase the disturbances as ten times as before, which is $B = 10 * \text{diag}([0.003, 0.004, 0.005, 0.006, 0.007, 0.008, 0.009, 0.01])$, the minimum and optimal power vector starting from the power supply vector [12, 12, 12]

Minimum	p_1	p_2	p_3	p_4	p_5	p_6	p_7	p_8
0.5429	11.7953	12.3226	13.3546	12.5275	-12	-12	-13	-13

Table 19: Increase the disturbances as ten times as before, which is $B = 10 * \text{diag}([0.003, 0.004, 0.005, 0.006, 0.007, 0.008, 0.009, 0.01])$, the minimum and optimal power vector starting from the power supply vector [11, 11, 14]

Minimum	p_1	p_2	p_3	p_4	p_5	p_6	p_7	p_8
1.0121	11.0830	12.0034	14.5491	12.3645	-12	-12	-13	-13

Table 20: Increase the line capacity to 35 and the disturbance vector into $B = 10 * \text{diag}([0.003, 0.004, 0.005, 0.006, 0.007 + 0.005, 0.008 + 0.005, 0.009 + 0.005, 0.01 + 0.005])$, the minimum and optimal power vector starting from the power supply vector [12, 12, 12]

Minimum	p_1	p_2	p_3	p_4	p_5	p_6	p_7	p_8
0.9543	8.4800	12.8453	13.4957	15.1790	-12	-12	-13	-13

Table 21: Increase the line capacity to 35 and the disturbance vector into $B = 10 * \text{diag}([0.003, 0.004, 0.005, 0.006, 0.007 + 0.005, 0.008 + 0.005, 0.009 + 0.005, 0.01 + 0.005])$, the minimum and optimal power vector starting from the power supply vector [11, 11, 14]

Minimum	p_1	p_2	p_3	p_4	p_5	p_6	p_7	p_8
0.9541	6.2285	13.6142	15.7461	14.4112	-12	-12	-13	-13

Table 22: Increase the line capacity to 35 and change the disturbance vector into $B = 10 * \text{diag}([0.008, 0.003, 0.01, 0.001, 0.015, 0.02, 0.018, 0.03])$, the minimum and optimal power vector starting from the power supply vector [12, 12, 12]

Minimum	p_1	p_2	p_3	p_4	p_5	p_6	p_7	p_8
1.2780	8.2883	7.7117	16.00	18	-12	-12	-13	-13

Table 23: Increase the line capacity to 35 and change the disturbance vector into $B = 10 * \text{diag}([0.008, 0.003, 0.01, 0.001, 0.015, 0.02, p.018, 0.03])$, the minimum and optimal power vector starting from the power supply vector [11, 11, 14]

Minimum	p_1	p_2	p_3	p_4	p_5	p_6	p_7	p_8
1.2768	1.9974	13.9974	15.9985	18.0067	-12	-12	-13	-13

3 Tables of a Manhattan-grid Network Example

The picture of a Manhattan-grid power network with 25 nodes is displayed in Fig. 2 where the nodes 1, 2, 3, 4 provide power supply and the other nodes model power demand. Table 26 shows the parameters of this network. In this example, we only change the power demand vector from a symmetric one to an asymmetric one, which leads to a symmetric or asymmetric optimal power supply vector in Tables 24 and 25, separately.

Tables 27 and 28 show the absolute value of mean of phase-angle difference: $|\theta_i - \theta_j|$, the standard deviation of the phase-angle difference of this power line: σ_{ij} , each component of the control objective vector: $|\theta_i - \theta_j| + 3.08\sigma_{ij}$ and power flow vector $l_{ij}\sin(|\theta_i - \theta_j| + 3.08\sigma_{ij})$, and these two tables are ordered by the values of $|\theta_i - \theta_j| + 3.08\sigma_{ij}$ in the descending order. As in the eight-node academic network, in contrast with the results in Table 25, the computation has been additionally been evaluated by discretizing the set of three power supply vectors for each dimension into a grid with 150 steps and the minimum is 1.3416, also slightly larger than the value computed by the descent procedure. Meanwhile, for this power network with large amount of nodes and links, the descent procedure has a higher efficiency than the partition method.

What's more, from Tables 27 and 28, one can see the total power demand of the neighborhood of a power supply node is much larger than the capacity of the line which connects the neighborhood with this power supply node, e.g. a neighborhood: node 5, 6, 7, 8, 9 and the connection line 1 – 7. If this power network is a tree-like network, it will lose transient stability immediately. But this power network remains very stable and this is due to its network structure and the number of links.

Furthermore, as for the eight-node example, the largest value and the second largest value of the vector $|\theta_i - \theta_j| + 3.08\sigma_{ij}$ differ very little. Moreover, the computations from different initial power supply vectors are considered, but they converge to similar minimizers. The reason maybe that although the strength of the disturbance in this example is much larger than that in eight-node academic example, the damping coefficients are also larger. Hence, to consider the convexity property of the control objective function, it is always necessary to consider the damping coefficients and the strengths of the disturbances together.

Last but not least, as the control objective of maintaining the phase-angle differences over power lines inside the critical set, is more important than the classical secondary frequency control with its emphasis on minimizing the economic cost. Therefore, a comparison is made of the performance of the power system without and with control. Here, we use the *proportional control law* as the form of without control. Results are shown in Tables 29 and 30 for symmetric power demand vector and symmetric disturbance vector. Then we change the strength of disturbance to be asymmetric, the results are shown in Tables 31 and 32. These four tables are ordered by the values of $|\theta_i - \theta_j| + 3.08 * \sigma_{ij}$. We can see the largest and the second largest values of $|\theta_i - \theta_j| + 3.08 * \sigma_{ij}$ decrease while the other values may go up and down. Moreover, a figure depicting the probability density function for the cases ‘without control’ and ‘with control’ of line 1 – 7 where the disturbance vector are asymmetric are presented, as illustrated in Fig. 3. Note that the values are borrowed from in Table 32. In this illustration, the reduction in both standard deviation and mean value from the ‘without control’ to the ‘with control’ condition is not readily apparent. This is attributed to the small magnitude of the decrease, making it challenging to discern in the visual representation.

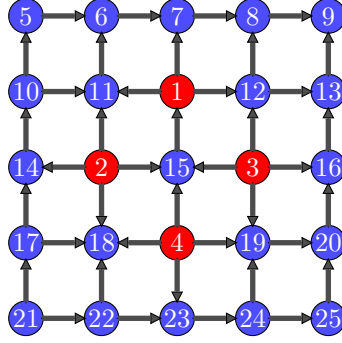


Figure 2: A Manhattan-grid network

Table 24: The minimum value and optimal power vector starting from the power supply vector [45,53,55] for a symmetric power demand vector

Minimum	p_1	p_2	p_3	p_4	p_5	p_6	p_7	p_8	p_9	p_{10}	p_{11}	p_{12}
1.4253	45.0000	60.0000	60.0000	45.0000	-9.5000	-14	-8	-14	-9.5	-8	-8	-8
p_{13}	p_{14}	p_{15}	p_{16}	p_{17}	p_{18}	p_{19}	p_{20}	p_{21}	p_{22}	p_{23}	p_{24}	p_{25}
-8	-14	-8	-14	-8	-8	-8	-8	-9.5	-14	-8	-14	-9.5

Table 25: The minimum value and optimal power vector starting from the power supply vector [45,53,55] for an asymmetric power demand vector

Minimum	p_1	p_2	p_3	p_4	p_5	p_6	p_7	p_8	p_9	p_{10}	p_{11}	p_{12}
1.3413	43.1692	60.0000	60.0000	46.8308	-5	-8	-8	-10	-8	-10	-14	-16
p_{13}	p_{14}	p_{15}	p_{16}	p_{17}	p_{18}	p_{19}	p_{20}	p_{21}	p_{22}	p_{23}	p_{24}	p_{25}
-8	-14	-14	-14	-8	-14	-14	-8	-8	-8	-8	-8	-5

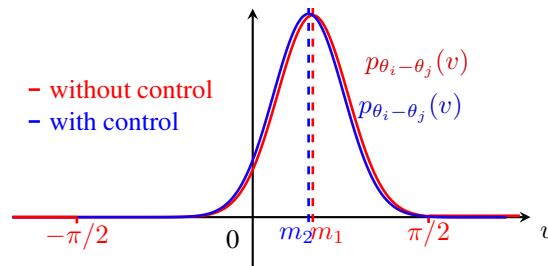


Figure 3: Example. Manhattan-grid network, line 1-7, without and with control, disturbance vector asymmetric.

Table 26: Network parameters in which the line capacity is not listed there, where all line capacities equal 40

Node i	$p^{+,max}$ $-p^{-,max}$ symmetric	$p^{+,max}$ $-p^{-,max}$ asymmetric	Inertia m_i	Damping d_i	Disturbance symmetric $K_2(i, i)$	Disturbance asymmetric $K_2(i, i)$
1	60	60	10	4	2	1.5682
2	60	60	10	4	2	2.0387
3	60	60	10	4	2	1.3929
4	60	60	10	4	2	1.4432
5	-9.5	-5	1	0	2	1.9966
6	-14	-8	1	0	2	2.7663
7	-8	-8	1	0	2	1.6152
8	-14	-10	1	0	2	2.1857
9	-9.5	-8	1	0	2	1.8872
10	-8	-10	1	1	2	2.5587
11	-8	-14	1	1	2	1.4555
12	-8	-16	1	1	2	2.0163
13	-8	-8	1	1	2	2.2763
14	-14	-14	1	1	2	2.5503
15	-8	-14	1	1	2	2.7721
16	-14	-14	1	1	2	2.0430
17	-8	-8	1	1	2	1.2542
18	-8	-14	1	1	2	1.6288
19	-8	-14	1	1	2	1.4692
20	-8	-8	1	1	2	3.1752
21	-9.5	-8	1	0	2	1.6922
22	-14	-8	1	0	2	2.3740
23	-8	-8	1	0	2	1.9038
24	-14	-8	1	0	2	2.4443
25	-9.5	-5	1	0	2	1.6176

Table 27: Phase-angle differences and other outputs, power demand vector symmetric, disturbance vector symmetric

i	j	$ \theta_i - \theta_j $	σ_{ij}	$ \theta_i - \theta_j + 3.08 \sigma_{ij}$	$l_{ij} \sin (\theta_i - \theta_j + 3.08 \sigma_{ij})$
1	7	0.5018	0.2998	1.4253	39.5773
4	23	0.5018	0.2998	1.4253	39.5773
2	14	0.5932	0.2418	1.3379	38.9200
3	16	0.5932	0.2418	1.3379	38.9200
2	18	0.4343	0.2160	1.0997	35.6429
3	19	0.4343	0.2160	1.0997	35.6429
2	11	0.4343	0.2160	1.0997	35.6429
3	12	0.4343	0.2160	1.0997	35.6429
8	9	0.0904	0.3246	1.0900	35.4652
5	6	0.0904	0.3246	1.0900	35.4652
24	25	0.0904	0.3246	1.0900	35.4652
21	22	0.0904	0.3246	1.0900	35.4652
18	22	0.3044	0.2399	1.0434	34.5643
19	24	0.3044	0.2399	1.0434	34.5643
6	11	0.3044	0.2399	1.0434	34.5643
8	12	0.3044	0.2399	1.0434	34.5643
7	8	0.1410	0.2905	1.0358	34.4114
6	7	0.1410	0.2905	1.0358	34.4114
23	24	0.1410	0.2905	1.0358	34.4114
22	23	0.1410	0.2905	1.0358	34.4114
1	12	0.3276	0.2221	1.0116	33.9063
1	11	0.3276	0.2221	1.0116	33.9063
4	19	0.3276	0.2221	1.0116	33.9063
4	18	0.3276	0.2221	1.0116	33.9063
12	13	0.2452	0.2468	1.0055	33.7763
10	11	0.2452	0.2468	1.0055	33.7763
19	20	0.2452	0.2468	1.0055	33.7763
17	18	0.2452	0.2468	1.0055	33.7763
17	21	0.1478	0.2699	0.9792	33.2026
20	25	0.1478	0.2699	0.9792	33.2026
5	10	0.1478	0.2699	0.9792	33.2026
9	13	0.1478	0.2699	0.9792	33.2026
14	17	0.1047	0.2622	0.9123	31.6369
16	20	0.1047	0.2622	0.9123	31.6369
10	14	0.1047	0.2622	0.9123	31.6369
13	16	0.1047	0.2622	0.9123	31.6369
2	15	0.0997	0.1506	0.5635	21.3651
3	15	0.0997	0.1506	0.5635	21.3651
1	15	5.0008e-04	0.1625	0.5010	19.2139
4	15	4.9992e-04	0.1625	0.5010	19.2139

Table 28: Phase-angle differences and other outputs, power demand vector asymmetric, disturbance vector symmetric

i	j	$ \theta_i - \theta_j $	σ_{ij}	$ \theta_i - \theta_j + 3.08 \sigma_{ij}$	$l_{ij} \sin(\theta_i - \theta_j + 3.08 \sigma_{ij})$
1	7	0.4285	0.2964	1.3413	38.9515
4	23	0.4285	0.2964	1.3413	38.9515
2	14	0.5614	0.2400	1.3004	38.5470
3	16	0.5547	0.2397	1.2929	38.4649
3	12	0.4742	0.2169	1.1423	36.3841
21	22	0.1100	0.3248	1.1103	35.8330
2	11	0.4453	0.2159	1.1102	35.8319
8	9	0.0910	0.3239	1.0886	35.4392
2	18	0.4155	0.2161	1.0810	35.2966
24	25	0.0722	0.3241	1.0704	35.0949
5	6	0.0703	0.3235	1.0668	35.0266
3	19	0.3984	0.2156	1.0624	34.9418
4	18	0.3529	0.2219	1.0363	34.4201
1	12	0.3477	0.2226	1.0333	34.3590
4	19	0.3410	0.2215	1.0231	34.1494
7	8	0.1334	0.2885	1.0219	34.1242
22	23	0.1203	0.2884	1.0086	33.8443
1	11	0.3154	0.2216	0.9980	33.6155
23	24	0.0957	0.2880	0.9827	33.2808
17	18	0.2110	0.2461	0.9691	32.9745
6	7	0.0826	0.2876	0.9683	32.9573
10	11	0.2046	0.2459	0.9619	32.8115
19	20	0.1971	0.2457	0.9539	32.6265
12	13	0.1907	0.2457	0.9475	32.4785
8	12	0.2094	0.2375	0.9407	32.3197
9	13	0.1094	0.2690	0.9378	32.2493
13	16	0.1199	0.2614	0.9251	31.9470
18	22	0.1910	0.2371	0.9213	31.8551
6	11	0.1889	0.2372	0.9193	31.8082
17	21	0.0903	0.2689	0.9184	31.7852
19	24	0.1775	0.2369	0.9071	31.5079
10	14	0.1018	0.2614	0.9070	31.5063
14	17	0.0808	0.2611	0.8849	30.9547
5	10	0.0548	0.2682	0.8809	30.8526
20	25	0.0529	0.2683	0.8792	30.8086
16	20	0.0571	0.2609	0.8605	30.3279
2	15	0.1337	0.1507	0.5978	22.5138
3	15	0.1291	0.1507	0.5934	22.3657
4	15	0.0753	0.1621	0.5744	21.7340
1	15	0.0128	0.1624	0.5131	19.6341

Table 29: Phase-angle differences and other outputs for Manhattan network with and without control, power demand vector symmetric, disturbance vector symmetric

control	i	j	$ \theta_i - \theta_j $	σ_{ij}	$ \theta_i - \theta_j + 3.08 \sigma_{ij}$	$l_{ij} \sin(\theta_i - \theta_j + 3.08 \sigma_{ij})$
without	1	7	0.5363	0.3017	1.4657	39.7793
with	1	7	0.5018	0.2998	1.4253	39.5773
without	4	23	0.5363	0.3017	1.4657	39.7793
with	4	23	0.5018	0.2998	1.4253	39.5773
without	2	14	0.5574	0.2408	1.2990	38.5317
with	2	14	0.5932	0.2418	1.3379	38.9200
without	13	16	0.0896	0.2618	0.8960	31.2337
with	3	16	0.5932	0.2418	1.3379	38.9200
without	2	18	0.3771	0.2161	1.0428	34.5527
with	2	18	0.4343	0.2160	1.0997	35.6429
without	3	19	0.3771	0.2161	1.0428	34.5527
with	3	19	0.4343	0.2160	1.0997	35.6429
without	2	11	0.3771	0.2161	1.0428	34.5527
with	2	11	0.4343	0.2160	1.0997	35.6429
without	3	12	0.3771	0.2161	1.0428	34.5527
with	3	12	0.4343	0.2160	1.0997	35.6429
without	8	9	0.0979	0.3242	1.0963	35.5810
with	8	9	0.0904	0.3246	1.0900	35.4652
without	5	6	0.0979	0.3242	1.0963	35.5810
with	5	6	0.0904	0.3246	1.0900	35.4652
without	24	25	0.0979	0.3242	1.0963	35.5810
with	24	25	0.0904	0.3246	1.0900	35.4652
without	21	22	0.0979	0.3242	1.0963	35.5810
with	21	22	0.0904	0.3246	1.0900	35.4652
without	18	22	0.2966	0.2401	1.0361	34.4178
with	18	22	0.3044	0.2399	1.0434	34.5643
without	19	24	0.2966	0.2401	1.0361	34.4178
with	19	24	0.3044	0.2399	1.0434	34.5643
without	6	11	0.2966	0.2401	1.0361	34.4178
with	6	11	0.3044	0.2399	1.0434	34.5643
without	8	12	0.2966	0.2401	1.0361	34.4178
with	8	12	0.3044	0.2399	1.0434	34.5643
without	7	8	0.1561	0.2910	1.0524	34.7451
with	7	8	0.1410	0.2905	1.0358	34.4114
without	6	7	0.1561	0.2910	1.0524	34.7451
with	6	7	0.1410	0.2905	1.0358	34.4114
without	23	24	0.1561	0.2910	1.0524	34.7451
with	23	24	0.1410	0.2905	1.0358	34.4114
without	22	23	0.1561	0.2910	1.0524	34.7451
with	22	23	0.1410	0.2905	1.0358	34.4114

Table 30: Continue of 29

control	i	j	$ \theta_i - \theta_j $	σ_{ij}	$ \theta_i - \theta_j + 3.08 \sigma_{ij}$	$l_{ij} \sin(\theta_i - \theta_j + 3.08 \sigma_{ij})$
without	1	12	0.3836	0.2225	1.0688	35.0655
with	1	12	0.3276	0.2221	1.0116	33.9063
without	1	11	0.3836	0.2225	1.0688	35.0655
with	1	11	0.3276	0.2221	1.0116	33.9063
without	4	19	0.3836	0.2225	1.0688	35.0655
with	4	19	0.3276	0.2221	1.0116	33.9063
without	4	18	0.3836	0.2225	1.0688	35.0655
with	4	18	0.3276	0.2221	1.0116	33.9063
without	12	13	0.2529	0.2468	1.0132	33.9414
with	12	13	0.2452	0.2468	1.0055	33.7763
without	10	11	0.2529	0.2468	1.0132	33.9414
with	10	11	0.2452	0.2468	1.0055	33.7763
without	19	20	0.2529	0.2468	1.0132	33.9414
with	19	20	0.2452	0.2468	1.0055	33.7763
without	17	18	0.2529	0.2468	1.0132	33.9414
with	17	18	0.2452	0.2468	1.0055	33.7763
without	17	21	0.1402	0.2697	0.9709	33.0156
with	17	21	0.1478	0.2699	0.9792	33.2026
without	20	25	0.1402	0.2697	0.9709	33.0156
with	20	25	0.1478	0.2699	0.9792	33.2026
without	5	10	0.1402	0.2697	0.9709	33.0156
with	5	10	0.1478	0.2699	0.9792	33.2026
without	9	13	0.1402	0.2697	0.9709	33.0156
with	9	13	0.1478	0.2699	0.9792	33.2026
without	14	17	0.0896	0.2618	0.8960	31.2337
with	14	17	0.1047	0.2622	0.9123	31.6369
without	16	20	0.0896	0.2618	0.8960	31.2337
with	16	20	0.1047	0.2622	0.9123	31.6369
without	10	14	0.0896	0.2618	0.8960	31.2337
with	10	14	0.1047	0.2622	0.9123	31.6369
without	13	16	0.0896	0.2618	0.8960	31.2337
with	13	16	0.1047	0.2622	0.9123	31.6369
without	2	15	0.0470	0.1506	0.5110	19.5606
with	2	15	0.0997	0.1506	0.5635	21.3651
without	3	15	0.0470	0.1506	0.5110	19.5606
with	3	15	0.0997	0.1506	0.5635	21.3651
without	1	15	0.0530	0.1622	0.5526	20.9973
with	1	15	5.0005e-04	0.1625	0.5010	19.2139
without	4	15	0.0530	0.1622	0.5526	20.9973
with	4	15	4.9995e-04	0.1625	0.5010	19.2139

Table 31: Phase-angle differences and other outputs for Manhattan network without and with control, power demand vector symmetric, disturbance vector asymmetric

control	i	j	$ \theta_i - \theta_j $	σ_{ij}	$ \theta_i - \theta_j + 3.08 \sigma_{ij}$	$l_{ij} \sin(\theta_i - \theta_j + 3.08 \sigma_{ij})$
without	1	7	0.5363	0.3149	1.5062	39.9165
with	1	7	0.4990	0.3128	1.4625	39.7656
without	4	23	0.5363	0.3128	1.4997	39.8990
with	4	23	0.5046	0.3110	1.4625	39.7656
without	3	16	0.5574	0.2589	1.3550	39.0719
with	3	16	0.5932	0.2601	1.3943	39.3787
without	2	14	0.5574	0.2590	1.3550	39.0725
with	2	14	0.5932	0.2600	1.3941	39.3770
without	5	6	0.0979	0.3412	1.1489	36.4920
with	5	6	0.0896	0.3416	1.1416	36.3717
without	8	9	0.0979	0.3377	1.1380	36.3114
with	8	9	0.0896	0.3381	1.1310	36.1934
without	3	12	0.3771	0.2233	1.0650	34.9921
with	3	12	0.4379	0.2233	1.1255	36.0993
without	2	11	0.3771	0.2218	1.0602	34.8979
with	2	11	0.4379	0.2214	1.1199	36.0019
without	19	24	0.2966	0.2631	1.1068	35.7715
with	19	24	0.3040	0.2628	1.1135	35.8899
without	24	25	0.0979	0.3304	1.1154	35.9243
with	24	25	0.0912	0.3307	1.1099	35.8256
without	6	11	0.2966	0.2599	1.0971	35.5958
with	6	11	0.3049	0.2597	1.1046	35.7320
without	3	19	0.3771	0.2182	1.0493	34.6824
with	3	19	0.4307	0.2180	1.1022	35.6882
without	21	22	0.0979	0.3275	1.1065	35.7661
with	21	22	0.0912	0.3279	1.1012	35.6696
without	6	7	0.1561	0.3109	1.1138	35.8953
with	6	7	0.1397	0.3104	1.0959	35.5731
without	8	12	0.2966	0.2549	1.0816	35.3077
with	8	12	0.3049	0.2547	1.0895	35.4555
without	23	24	0.1561	0.3071	1.1019	35.6832
with	23	24	0.1422	0.3068	1.0870	35.4102
without	7	8	0.1561	0.3068	1.1010	35.6670
with	7	8	0.1397	0.3062	1.0829	35.3328
without	2	18	0.3771	0.2113	1.0278	34.2468
with	2	18	0.4307	0.2112	1.0812	35.3018
without	10	11	0.2529	0.2681	1.0787	35.2529
with	10	11	0.2439	0.2681	1.0695	35.0792

Table 32: Continue of page 31

control	i	j	$ \theta_i - \theta_j $	σ_{ij}	$ \theta_i - \theta_j + 3.08 \sigma_{ij}$	$l_{ij} \sin(\theta_i - \theta_j + 3.08 \sigma_{ij})$
without	22	23	0.1561	0.3016	1.0849	35.3708
with	22	23	0.1422	0.3011	1.0695	35.0788
without	19	20	0.2529	0.2672	1.0759	35.2016
with	19	20	0.2465	0.2672	1.0694	35.0757
without	12	13	0.2529	0.2614	1.0582	34.8588
with	12	13	0.2439	0.2615	1.0495	34.6861
without	18	22	0.2966	0.2415	1.0404	34.5038
with	18	22	0.3040	0.2414	1.0475	34.6473
without	1	12	0.3836	0.2299	1.0916	35.4955
with	1	12	0.3233	0.2295	1.0302	34.2956
without	20	25	0.1402	0.2863	1.0220	34.1257
with	20	25	0.1470	0.2866	1.0297	34.2848
without	1	11	0.3836	0.2285	1.0874	35.4173
with	1	11	0.3233	0.2281	1.0259	34.2074
without	4	19	0.3836	0.2253	1.0776	35.2324
with	4	19	0.3319	0.2250	1.0250	34.1878
without	9	13	0.1402	0.2836	1.0137	33.9513
with	9	13	0.1486	0.2837	1.0224	34.1340
without	17	18	0.2529	0.2494	1.0211	34.1071
with	17	18	0.2465	0.2495	1.0149	33.9772
without	5	10	0.1402	0.2800	1.0026	33.7152
with	5	10	0.1486	0.2803	1.0119	33.9140
without	4	18	0.3836	0.2184	1.0562	34.8204
with	4	18	0.3319	0.2180	1.0033	33.7302
without	16	20	0.0896	0.2848	0.9667	32.9210
with	16	20	0.1026	0.2852	0.9809	33.2407
without	10	14	0.0896	0.2810	0.9552	32.6562
with	10	14	0.1068	0.2813	0.9731	33.0644
without	13	16	0.0896	0.2795	0.9506	32.5503
with	13	16	0.1068	0.2799	0.9689	32.9717
without	17	21	0.1402	0.2644	0.9547	32.6449
with	17	21	0.1470	0.2647	0.9621	32.8154
without	14	17	0.0896	0.2713	0.9252	31.9498
with	14	17	0.1026	0.2717	0.9396	32.2931
without	2	15	0.0470	0.1859	0.6197	23.2325
with	2	15	0.0997	0.1859	0.6723	24.9118
without	3	15	0.0470	0.1854	0.6181	23.1804
with	3	15	0.0997	0.1854	0.6706	24.8577
without	4	15	0.0530	0.1928	0.6468	24.1064
with	4	15	0.0079	0.1931	0.6025	22.6696
without	1	15	0.0530	0.1928	0.6468	24.1067
with	1	15	0.0069	0.1932	0.6018	22.6465

4 Tables of a Ring Network Example

The picture of the twelve-node ring network is displayed in Fig. 4. First, a group of symmetric parameters are shown in 33 which leads to the symmetric outputs in Tables 34 and 35. From the three columns of $|\theta_i - \theta_j|$, σ_{ij} , $|\theta_i - \theta_j| + 3.08\sigma_{ij}$ in Table 35, one can see that several transmission lines have very small almost zero power flows but at the same time their fluctuations are serious. Thus, it is necessary to consider both the mean value and the standard deviation of the phase-angle difference together.

Secondly, several of the parameters are changed to be asymmetric as shown in Tables 36 and 37. The computation results are exhibited in Tables 38 and 39 starting from the power supply vector $[20, 28, 15]$ and in Tables 40 and 41 starting from the power supply vector $[23, 19, 24]$. From these four tables, one can see that the lines which connect two neighbourhoods have now small power flows. What's more, the two different initial points lead to almost the same minimizers. The numerical results verify our conjecture again that compared with the damping coefficients, the strength of disturbances are not large enough, which results in the local minimizers of the control objective function are quite close to each other .

Moreover, as for the Manhattan network, the performances with values for without and with control are shown in Table 42. Then we increase the strengths of the disturbances to be 1.5 times the values of Table 36 to make the network parameter more realistic, the performances for without and for with control are shown in Table 43. In Tables 42 and 43, it is observable that the two highest values of $|\theta_i - \theta_j| + 3.08\sigma_{ij}$ have slightly decreased as well. Similar to the Manhattan-grid network, we generate a figure portraying the probability density function for both the ‘without control’ and ‘with control’ scenarios of line 1 – 12, as shown in Fig. 5, where the values are borrowed from Table 43. In this depiction, the discernible reduction in both standard deviation and mean value from the ‘without control’ to the ‘with control’ condition is now evident.

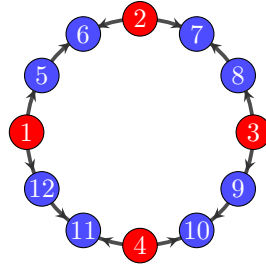


Figure 4: A ring network

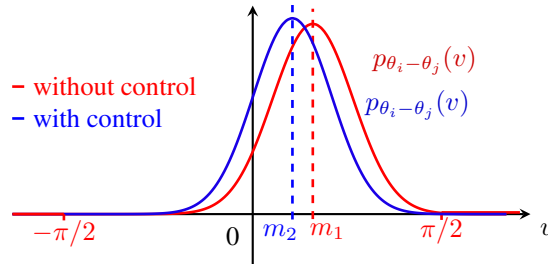


Figure 5: Example. ring network, line 1-12, without and with control.

Table 33: Network parameters, where the line capacities are not shown and they are all equal 30.

Node i	$p^{+,max},$ $-p^{-,max}$	Inertia m_i	Damping d_i	Disturbance $K_2(i, i)$
1	30	10	2	2
2	20	10	2	2
3	25	10	2	2
4	20	10	2	2
5	-10	1	1	2
6	-10	1	1	2
7	-10	1	1	2
8	-10	1	1	2
9	-10	1	1	2
10	-10	1	1	2
11	-10	1	1	2
12	-10	1	1	2

Table 34: The minimum and optimal power vector starting from the power supply vector [20,18,25]

Minimum	p_1	p_2	p_3	p_4	p_5	p_6	p_7	p_8	p_9	p_{10}	p_{11}	p_{12}
1.0469	19.9968	19.9974	20.0059	20.0000	-10	-10	-10	-10	-10	-10	-10	-10

Table 35: Phase-angle differences and other outputs

i	j	$ \theta_i - \theta_j $	σ_{ij}	$ \theta_i - \theta_j + 3.08 \sigma_{ij}$	$l_{ij} \sin(\theta_i - \theta_j + 3.08 \sigma_{ij})$
3	8	0.3400	0.2295	1.0469	25.9758
3	9	0.3399	0.2295	1.0468	25.9751
4	11	0.3399	0.2295	1.0468	25.9751
2	6	0.3399	0.2295	1.0468	25.9743
1	5	0.3398	0.2295	1.0467	25.9732
1	12	0.3398	0.2295	1.0466	25.9725
4	10	0.3398	0.2295	1.0466	25.9725
2	7	0.3397	0.2295	1.0466	25.9717
7	8	1.1989e-04	0.2252	0.6938	19.1831
9	10	7.6249e-05	0.2252	0.6937	19.1821
11	12	7.5869e-05	0.2252	0.6937	19.1821
5	6	3.2226e-05	0.2252	0.6937	19.1811

Changing the parameters: Several parameters are changed to be asymmetric.

Table 36: Network parameters

Node i	$p^{+,max},$ $-p^{-,max}$	Inertia m_i	Damping d_i	Disturbance $K_2(i, i)$
1	30	10	2	2.00
2	20	10	2	2.30
3	25	10	2	2.50
4	20	10	2	2.70
5	-6	1	1	1.60
6	-10	1	1	1.70
7	-8	1	1	1.80
8	-12	1	1	1.90
9	-17	1	1	1.65
10	-13	1	1	1.75
11	-7	1	1	1.85
12	-11	1	1	2.05

Table 37: Line capacities

l_{1-5}	l_{1-12}	l_{2-6}	l_{2-7}	l_{3-8}	l_{3-9}	l_{4-10}	l_{4-11}	l_{5-6}	l_{7-8}	l_{9-10}	l_{11-12}
30	32	34	36	38	40	31	33	35	37	39	35

Table 38: The minimum value and optimal power vector starting from the power supply vector [20,18,25]

Minimum	p_1	p_2	p_3	p_4	p_5	p_6	p_7	p_8	p_9	p_{10}	p_{11}	p_{12}
1.0674	19.9368	20.0002	25.0001	19.0628	-6	-10	-8	-12	-17	-13	-7	-11

Table 39: Phase-angle differences and other outputs

i	j	$ \theta_i - \theta_j $	σ_{ij}	$ \theta_i - \theta_j + 3.08 \sigma_{ij}$	$l_{ij} \sin(\theta_i - \theta_j + 3.08 \sigma_{ij})$
4	10	0.4440	0.2024	1.0674	27.1548
1	12	0.3929	0.2185	1.0659	28.0076
3	9	0.4303	0.1833	0.9947	33.5439
2	7	0.3306	0.1958	0.9337	28.9369
1	5	0.2590	0.1941	0.8568	22.6721
4	11	0.1751	0.2110	0.8250	24.2400
2	6	0.2471	0.1851	0.8171	24.7909
3	8	0.2206	0.1906	0.8076	27.4596
7	8	0.0997	0.1917	0.6902	23.5578
11	12	0.0358	0.2063	0.6713	21.7690
5	6	0.0481	0.1803	0.6035	19.8648
9	10	0.0081	0.1767	0.5524	20.4643

Table 40: The minimum value and optimal power vector starting from the power supply vector [23,19,24]

Minimum	p_1	p_2	p_3	p_4	p_5	p_6	p_7	p_8	p_9	p_{10}	p_{11}	p_{12}
1.0670	19.9749	20.0000	25.0000	19.0250	-6	-10	-8	-12	-17	-13	-7	-11

Table 41: Phase-angle differences and other outputs

i	j	$ \theta_i - \theta_j $	σ_{ij}	$ \theta_i - \theta_j + 3.08 \sigma_{ij}$	$l_{ij} \sin(\theta_i - \theta_j + 3.08 \sigma_{ij})$
4	10	0.4436	0.2024	1.0670	27.1490
1	12	0.3939	0.2185	1.0670	28.0239
3	9	0.4305	0.1833	0.9950	33.5504
2	7	0.3308	0.1958	0.9340	28.9436
1	5	0.2594	0.1941	0.8571	22.6792
4	11	0.1742	0.2110	0.8241	24.2202
2	6	0.2468	0.1851	0.8167	24.7833
3	8	0.2203	0.1906	0.8073	27.4523
7	8	0.1000	0.1917	0.6905	23.5656
11	12	0.0366	0.2063	0.6721	21.7912
5	6	0.0484	0.1803	0.6038	19.8732
9	10	0.0078	0.1767	0.5521	20.4560

Table 42: Phase-angle differences and other outputs for ring network without and with control

control	i	j	$ \theta_i - \theta_j $	σ_{ij}	$ \theta_i - \theta_j + 3.08 \sigma_{ij}$	$l_{ij} \sin(\theta_i - \theta_j + 3.08 \sigma_{ij})$
without	4	10	0.5055	0.2051	1.1371	28.1300
with	4	10	0.4436	0.2024	1.0670	27.1490
without	1	12	0.4995	0.2229	1.1862	29.6623
with	1	12	0.3939	0.2185	1.0670	28.0239
without	3	9	0.3840	0.1820	0.9447	32.4125
with	3	9	0.4305	0.1833	0.9950	33.5504
without	2	7	0.3659	0.1968	0.9721	29.7379
with	2	7	0.3308	0.1958	0.9340	28.9436
without	1	5	0.3825	0.1971	0.9897	25.0764
with	1	5	0.2594	0.1941	0.8571	22.6792
without	4	11	0.0810	0.2108	0.7303	22.0145
with	4	11	0.1742	0.2110	0.8241	24.2202
without	2	6	0.1417	0.1837	0.7074	22.0945
with	2	6	0.2468	0.1851	0.8167	24.7833
without	3	8	0.1884	0.1902	0.7743	26.5697
with	3	8	0.2203	0.1906	0.8073	27.4523
without	7	8	0.1323	0.1921	0.7241	24.5118
with	7	8	0.1000	0.1917	0.6905	23.5656
without	11	12	0.1240	0.2070	0.7617	24.1551
with	11	12	0.0366	0.2063	0.6721	21.7912
without	5	6	0.1491	0.1813	0.7076	22.7494
with	5	6	0.0484	0.1803	0.6038	19.8732
without	9	10	0.0516	0.1769	0.5965	21.9087
with	9	10	0.0078	0.1767	0.5521	20.4560

Table 43: Change the strength of the disturbance to be 1.5 times that of 36, phase-angle differences and other outputs for ring network without and with control

control	i	j	$ \theta_i - \theta_j $	σ_{ij}	$ \theta_i - \theta_j + 3.08 \sigma_{ij}$	$l_{ij} \sin(\theta_i - \theta_j + 3.08 \sigma_{ij})$
without	4	10	0.5055	0.3076	1.4529	30.7847
with	4	10	0.4041	0.3015	1.3328	30.1261
without	1	12	0.4995	0.3344	1.5295	31.9727
with	1	12	0.3302	0.3248	1.3307	31.0824
without	3	9	0.3840	0.2730	1.2250	37.6323
with	3	9	0.4615	0.2764	1.3127	38.6754
without	2	7	0.3659	0.2952	1.2751	34.4379
with	2	7	0.3638	0.2951	1.2727	34.4118
without	2	6	0.1417	0.2755	0.9902	28.4286
with	2	6	0.3667	0.2819	1.2350	32.1007
without	4	11	0.0810	0.3162	1.0550	28.7060
with	4	11	0.2331	0.3175	1.2110	30.8875
without	3	8	0.1884	0.2853	1.0672	33.2825
with	3	8	0.1904	0.2853	1.0691	33.3175
without	7	8	0.1323	0.2882	1.0200	31.5284
with	7	8	0.1304	0.2881	1.0177	31.4836
without	1	5	0.3825	0.2957	1.2933	28.8527
with	1	5	0.1274	0.2886	1.0162	25.5027
without	11	12	0.1240	0.3106	1.0805	30.8774
with	11	12	0.0178	0.3095	0.9711	28.8919
without	5	6	0.1491	0.2720	0.9868	29.1996
with	5	6	0.0626	0.2705	0.8957	27.3222
without	9	10	0.0516	0.2654	0.8690	29.7824
with	9	10	0.0208	0.2651	0.8373	28.9706